Contents (Appendix)

A Optimizers

As we explained in Section 4.1, we compared SGD, momentum-SGD, Nesterov momentum, RMSprop, and Adam. We write the algorithm of these optimizers below.

A.1 SGD

$$\boldsymbol{\theta}_t \leftarrow \boldsymbol{\theta}_{t-1} - \eta_t \tilde{\nabla}_{\boldsymbol{\theta}_{t-1}} \ell\left(\boldsymbol{\theta}_{t-1}\right) \tag{2}$$

A.2 Momentum-SGD

$$\boldsymbol{v}_t \leftarrow \gamma \boldsymbol{v}_{t-1} + \eta_t \tilde{\nabla}_{\boldsymbol{\theta}_{t-1}} \ell\left(\boldsymbol{\theta}_{t-1}\right) \tag{3}$$

$$\boldsymbol{\theta}_t \leftarrow \boldsymbol{\theta}_{t-1} - \boldsymbol{v}_t \tag{4}$$

A.3 Nesterov Momentum

$$\boldsymbol{v}_t \leftarrow \gamma \boldsymbol{v}_{t-1} + \eta_t \tilde{\nabla}_{\boldsymbol{\theta}_{t-1}} \ell\left(\boldsymbol{\theta}_{t-1} - \gamma \boldsymbol{v}_{t-1}\right) \tag{5}$$

$$\boldsymbol{\theta}_t \leftarrow \boldsymbol{\theta}_{t-1} - \boldsymbol{v}_t \tag{6}$$

A.4 RMSprop

$$\boldsymbol{v}_t \leftarrow \alpha \boldsymbol{v}_{t-1} + (1-\alpha) \tilde{\nabla}_{\boldsymbol{\theta}_{t-1}} \ell\left(\boldsymbol{\theta}_t\right)^2 \tag{7}$$

$$\boldsymbol{m}_t \leftarrow \gamma \boldsymbol{m}_{t-1} + \frac{\eta_t}{\sqrt{\boldsymbol{v}_t + \epsilon}} \tilde{\nabla}_{\boldsymbol{\theta}_{t-1}} \ell\left(\boldsymbol{\theta}_t\right) \tag{8}$$

$$\boldsymbol{\theta}_t \leftarrow \boldsymbol{\theta}_{t-1} - \boldsymbol{m}_t \tag{9}$$

A.5 Adam

$$\boldsymbol{m}_t \leftarrow \beta_1 \boldsymbol{m}_{t-1} + \left(1-\beta_1\right) \tilde{\nabla}_{\boldsymbol{\theta}_{t-1}} \ell\left(\boldsymbol{\theta}_t\right) \tag{10}$$

$$\boldsymbol{v}_t \leftarrow \beta_2 \boldsymbol{v}_{t-1} + \left(1-\beta_2\right) \tilde{\nabla}_{\boldsymbol{\theta}_{t-1}} \ell\left(\boldsymbol{\theta}_t\right)^2 \tag{11}$$

$$b_t \leftarrow \frac{\sqrt{1-\beta_2^t}}{1-\beta_1^t} \tag{12}$$

$$\boldsymbol{\theta}_t \leftarrow \boldsymbol{\theta}_{t-1} - \eta_t \frac{\boldsymbol{m}_t}{\sqrt{\boldsymbol{v}_t} + \epsilon} b_t. \tag{13}$$

B Implementation and Environment for Experiments

We perform our experiment with supercomputer A (This name will be deanonymized when publication). For supercomputer A, each node is composed of NVIDIA Tesla V100×4GPU and Intel Xeon Gold 6148 2.4 GHz, 20 Cores×2CPU. As a software environment, we use Red Hat 4.8.5, gcc 7.4, Python 3.6.5, Pytorch 1.6.0, cuDNN 7.6.2, and CUDA 10.0.

All codes for experiments are modifications of the codes provided by the authors who introduced the datasets Gulrajani & Lopez-Paz (2021); Koh et al. (2021); Xiao et al. (2021). Licenses of the codes are MIT license for DomainBed Gulrajani & Lopez-Paz (2021) and WILDS Koh et al. (2021). The code of Backgrounds Challenge does not indicate the license. Our code can be found at the link below.
https://anonymous.4open.science/r/OoD-Optimizer-Comparison-37DF

C Datasets

C.1 DomainBed

DomainBed consists of sub-datasets shown in Table 2, where we exclude Terra Incognita and Rotated MNIST as stated in Section 3.2. We summarize the dataset information in the Table by referring to (Gulrajani & Lopez-Paz, 2021).

Table 2: DomainBed: Dataset Information

	domain	examples	class
Colored MNIST	[0.1, 0.2, 0.9]	70000	2
Rotated MNIST	[0, 15, 30, 45, 60, 75]	70000	10
PACS	[art, cartoons, photos, sketches]	9991	7
VLCS	[Caltech101, LabelMe,415SUN09, VOC2007]	10729	5
Office-Home	[art, clipart, product, real]	15588	65
TerraIncognita	[L100, L38, L43, L46]	24788	10
DomainNet	[clipart, infograph, painting, quickdraw,420real, sketch]	586575	345

Colored MNIST is a dataset for binary classification of MNIST dataset (Arjovsky et al., 2019). The digits from 0 to 4 are labeled 0, and those greater than 5 are labeled 1, and the task is to classify these classes successfully. However, each digit is also colored by either red or green. This is for having models to confuse the important feature for classification. The domain d indicates the correlation of the label with color. For example, if the domain is 0.1, the correlation between, say red, with the number smaller than 5 is 0.1. Furthermore, the label is flipped at a constant rate: in this paper, 15 % label is flipped. Therefore, the correlation between color and digit is d, while between label and digits is 0.85. That is, what models should learn is the correlation between label and noise, resulting in classification accuracy of 0.85. However, if the model exploits spurious correlation of the domain, it will learn the correlation between label and color, resulting in training accuracy being 0.9 but test accuracy being 0.1 in this case.

PACS and Office-Home are image datasets whose domain determines the style of the image. These are benchmark datasets for domain generalization.

VLCS is a set of different photographic datasets, PASCAL VOC (Everingham et al., 2010), LabelMe (Russell et al., 2008), Caltech101 (Fei-Fei et al., 2004), and SUN09 (Choi et al., 2010). PASCAL VOC, LabelMe, and SUN09 are benchmark datasets for object detection. Caltech101 is 101 classes image datasets, where each class has 40 - 80 samples.

DomainNet is a large dataset proposed for the study of domain generalization. The number of classes, domains, and dataset size is the largest in the DomainBed dataset.

TerraIncognita is a dataset consisting of images taken by cameras at different locations. The difference in the camera's location corresponds to the difference in the domain.

RotatedMNIST is a dataset that artificially rotates MNIST and divides the domain according to the rotation angle. The number in the domain corresponds to the rotation angle.

We leave one domain for the final evaluation and use the remaining domains for training. To evaluate the performance during training, we split the data of each domain into training data and validation data. The split ratio is 80 % for training and 20 % for validation. We take an average of test accuracies and validation accuracies across domains, respectively, and use them to evaluate the OOD generalization.

C.2 Backgrounds Challenge Dataset

In Section D.2, we explained that we use the subset of ImageNet (ORIGINAL). ORIGINAL consists of nine classes displayed in table 3. These classes are synthetically created from ImageNet classes based on WordNet ID. This table is a copy of a table in the original paper (Xiao et al., 2021).

Table 3: Backgrounds Challenge: Dataset information originally created in (Xiao et al., 2021)

classes	WordNet ID	num sub-classes
Dog	n02084071	116
Bird	n01503061	52
Vehicle	n04576211	42
Reptile	n01661091	36
Carnivore	n02075296	35
Insect	n02159955	27
Instrument	n03800933	26
Primate	n02469914	20
Fish	n02512053	16

This dataset is filtered to balance samples across classes. We follow the same filtering procedure as the original paper. For further details, please refer to the original paper (Xiao et al., 2021).

C.3 Amazon-WILDS and CivilComments-WILDS Dataset

WILDS is a set ob benchmark datasets with distributional shift and their variants: iWildCam (Beery et al., 2020), Camelyon17 (Bandi et al., 2018), RxRx1 (Taylor et al., 2019), OGB-MolPCBA (Hu et al., 2020), GlobalWheat (David et al., 2020; 2021), CivilComments (Borkan et al., 2019), FMoW (Christie et al., 2018), PovertyMap (Yeh et al., 2020), Amazon (Ni et al., 2019), and Py150 (Lu et al., 2021; Raychev et al., 2016). We use CivilComments and Amazon for our experiment as NLP tasks.

C.4 CIFAR10-C and CIFAR10-P Dataset

First, for the corrupted or perturbed data generalization studies, we use CIFAR-10-C, CIFAR-10-P to evaluate the generalization performance Hendrycks & Dietterich (2019); Mu & Gilmer (2019). CIFAR-10-C consist of CIFAR image data corrupted by 19 noise patterns. CIFAR-10-P is similar, but with ten perturbations. Similar corruptions and perturbations frequently occur in real-world imaging applications. Thus, evaluating the robustness against this noise is essential for improving practical applicability. Because noises changes the input samples, we can regard the corrupted and perturbed data as being sampled from a different distribution $P(\boldsymbol{x}, y)'$ than the original distribution: $P(\boldsymbol{x}, y)' \neq P(\boldsymbol{x}, y)$. If a classifier $f : \mathcal{X} \to \mathcal{Y}$ is robust to corruption $c : \mathcal{X} \to \mathcal{X}$, or $\mathbb{E}_{c \sim C}\left[P(f(c(\boldsymbol{x}) = y))\right]$ with corruption distribution C, we can say that the classifier can generalize for the corrupted samples. The same is true for perturbation.

D Experimental Protocol

We employ a Bayesian hyperparameter search strategy in the sweep functionality of Weights&Biases[5]. In this strategy, the relationship between parameters and evaluation metrics is modeled as a Gaussian process, and the parameters are selected in such a way as to optimize the improvement probability. Table 4 shows the number of hyperparameter optimizations performed for each task. The transition of the best ood accuracy in these hyperparameter optimizations is shown in Appendix G.2.

In line with previous studies (Gulrajani & Lopez-Paz, 2021; Xiao et al., 2021; Koh et al., 2021) different benchmarks use different evaluation metrics, each of which is outlined in the following sections.

Table 4: Number of Experiments for Each Dataset

	SGD	Momentum	Nesterov	RMSprop	Adam
RotatedMNIST	200	200	200	200	200
ColoredMNIST	200	342	200	200	200
PACS	200	200	200	200	412
VLCS	200	200	200	200	324
OfficeHome	399	200	200	200	699
TerraIncognita	200	200	200	451	202
DomainNet	490	515	857	1160	1137
Amazon-WILDS	440	438	449	489	466
Amazon-CivilComments	594	543	588	575	554
Background Challenge	-	347	-	-	567

D.1 DomainBed

We follow the setting that is employed in the original paper (Gulrajani & Lopez-Paz, 2021). We train models with training domains and evaluate their performance on the test domain, which is the domain not used for training. We use ResNet-50 for PACS, VLCS, Office-Home, DomainNet, TerraIncognita, and MNIST ConvNet (Gulrajani & Lopez-Paz, 2021) for RotatedMNIST and Colored MNIST.

In our experiments, one domain is used as the test domain (OOD: out-of-distribution) and the other domain as the training domain (ID: in-distribution). More precisely, the test domain is *"Art"* for PACS, *"Caltech101"* for VLSC, *"Art"* for Office-Home, *"Clipart"* for DomainNet, *"L100"* for TerraIncognita, "30°" for RotatedMNIST, and *"-90%"* for ColoredMNIST. We explain the experimental configurations in Section E.1.

D.2 Backgrounds Challenge Dataset

We follow Xiao et al. (2021) for using Backgrounds Challenge dataset for evaluation. Thus, we use the following data-generating procedure proposed by Xiao et al. (2021). We train ResNet-50 on ImageNet-1k with two popular optimizers, Momentum SGD, and Adam. The test datasets to evaluate the trained model are derivations of ImageNet dataset. First, we construct a subset of the ImageNet which has nine coarse-grained classes, e.g. insect (*ORIGINAL*). Especially, we refer to ORIGINAL with all images from ImageNet as *IN9L*. Then, we create a dataset by changing the background of the images of IN9L. In particular, we change the background of each image into a random background cropped from another image in ORIGINAL. We call this dataset *Mixed-Random*, following Xiao et al. (2021). By comparing the accuracy of Mixed-Same with that of ORIGINAL, we can measure the dependence of the model on the spurious correlation of background information. Thus, we investigate the relations between these two accuracies. The search range for hyperparameters is shown in Section E.2.

[5] https://wandb.ai/site

D.3 WILDS

We also follow the setting that is employed in the original paper (Koh et al., 2021). First, we divide the dataset into train, validation, and test and train a model using the train data. For model selection, we use the performance evaluation of validation data. In the test dataset, considering the subpopulation shift, we measure the performance of the OOD in the worst group for CivilComments-WILDS and in the domain of 10-percentile for Amazon-WILDS. In both Amazon-WILDS and CivilComments-WILDS, DistilBERT (Sanh et al., 2019) is used as the deep neural network model architecture. We explain the further details of the experimental configurations in Section E.3.

D.4 CIFAR10-C and CIFAR10-P

First, we trained deep neural networks with CIFAR-10[6]. Then we evaluated the trained models with CIFAR-10-C, CIFAR-10-P[7]. For the corruption datasets (CIFAR-10-C), we compared the accuracy for the corruption or perturbation test samples (samples from CIFAR-10-C) with that for the training domain test samples (samples from CIFAR-10). For the perturbation dataset, we measured the perturbation robustness introduced by Hendrycks & Dietterich (2019).

[6] https://www.cs.toronto.edu/~kriz/cifar.html
[7] https://zenodo.org/record/2535967

E Hyperparameters and Detailed Configurations

We report the hyperparameter's search space. For vanilla SGD, we search learning rate η, learning rate decay rate ρ and the timing to decay learning rate δ, and regularization coefficient of weight decay λ. When $\delta = 0.7$, it means that the learning rate decays when training passes 70 % of the total iterations. We do not search ρ and δ for DomainBed because we do not employ a learning rate schedule.

For non-adaptive momentum methods, a parameter to control momentum γ is added to the hyperparameters. For RMSprop, we further add parameters α and ϵ, which control the second-order momentum and numerical stability, respectively. Although ϵ is originally introduced for numerical stability, this parameter is found to play a crucial role in generalization performance (Choi et al., 2019). Thus, we follow Choi et al. and vary this parameter as well.

For Adam, we add ϵ, β_1, β_2 to vanilla SGD's configuration. The parameter ϵ is the same as that for RMSprop and β_1 and β_2 control first and second-order momentum terms, respectively.

E.1 DomainBed

We conduct Bayesian optimization for hyperparameter search of DomainBed. First, we sampled hyperparameters from uniform distribution whose minimum and maximum values are shown in the table 6 and 7 Then, we conducted Bayesian optimization on these sampled candidate hyperparameters and selected some of the hyperparameters among them. For reference, the scatter plot of Adam's learning rate for the OfficeHome dataset is shown in Appendix H.1. Note that the values for batch size B in the tables do not indicate minimum and maximum for Bayesian optimization but those for grid search. Unlike other datasets, we implement IRMv1 in addition to ERM. IRMv1 is a heuristic optimization problem to solve IRM, introduced by Arjovsky et al. (2019). Thus, we search the hyperparameters of IRMv1 as well.

IRMv1 is the following constrained optimization problem (Arjovsky et al., 2019):

$$\min_{\Phi:\mathcal{X}\to\mathcal{Y}} \sum_{e\in\mathcal{E}_{\text{tr}}} R^e(\Phi) + \lambda_{\text{IRM}} \left\|\nabla_{w|w=1.0} R^e(w\circ\Phi)\right\|^2, \tag{14}$$

where Φ is representation function and w is the weight on top of the function of a model $f = w \circ \Phi$. $\mathcal{X}$ is the input domain and $\mathcal{Y}$ is the output domain. The character e indicates an environment in training environment set $\mathcal{E}_{\text{tr}}$ and R^e is the risk of the environment. Because this is the optimization with regularization term, we search coefficient λ_{IRM}. In addition, we implement annealing of this coefficient and so we try various penalty annealing iterations N_{IRM} too. The basic workload is summarized in table 5.

We made two changes to the experimental setup in the original paper, as well as to the optimizer. We added regularization to the training of ColoredMNIST and RotatedMNIST to stabilize the learning. In addition, we increased the steps budget for RotatedMNIST because we observed that the training loss of RotatedMNIST was not sufficiently reduced.

We also experimented with two additional model architectures (ResNet-20 and Vision Transformer) for the benchmarks proposed in the existing DomainBed.

Table 5: DomainBed: Workloads

Model	Dataset	Batch size	Step Budget
MNIST ConvNet (Gulrajani & Lopez-Paz, 2021)	Colored MNIST	[128, 512, 2048]	5000
MNIST ConvNet (Gulrajani & Lopez-Paz, 2021)	Rotated MNIST	[128, 512, 2048]	100K
ResNet-50	VLCS	[64, 128]	5000
ResNet-50	PACS	[64, 128]	5000
ResNet-50	Office Home	[64, 128]	5000
ResNet-50	DomainNet	[64, 128]	5000
ResNet-50	TerraIncognita	[64, 128]	5000
Vision Transformer (for Additional Study)	PACS	[64]	5000
ResNet-20 (for Additional Study)	Colored MNIST	[64]	5000

Table 6: DomainBed: ResNet-50

	B	η	λ	γ	α	ϵ	λ_{IRM}	N_{IRM}
SGD	[64, 128]	[1e-5, 1e-2]	[1e-6, 1e-2]	-	-	-	[1e-1, 1e+5]	[1e+0, 1e+4]
Momentum	[64, 128]	[1e-5, 1e-2]	[1e-6, 1e-2]	[0, 0.99999]	-	-	[1e-1, 1e+5]	[1e+0, 1e+4]
Nesterov	[64, 128]	[1e-5, 1e-2]	[1e-6, 1e-2]	[0, 0.99999]	-	-	[1e-1, 1e+5]	[1e+0, 1e+4]
RMSprop	[64, 128]	[1e-5, 1e-2]	[1e-6, 1e-2]	[0, 0.99999]	[0, 0.999]	[1e-8, 1e-3]	[1e-1, 1e+5]	[1e+0, 1e+4]

	B	η	λ	β_1	β_2	ϵ	λ_{IRM}	N_{IRM}
Adam	[64, 128]	[1e-5, 1e-2]	[1e-6, 1e-2]	[0, 0.999]	[0, 0.999]	[1e-8, 1e-3]	[1e-1, 1e+5]	[1e+0, 1e+4]

	B	η	γ	ϵ	ρ
SAM	[64]	[1e-5, 1e-2]	[0.9]	[1e-4]	[5e-2]

Table 7: DomainBed: MNIST ConvNet (Gulrajani & Lopez-Paz, 2021)

	B	η	λ	γ	α	ϵ	λ_{IRM}	N_{IRM}
SGD	[128, 521, 2048]	[1e-5, 1e-2]	[1e-6, 1e-2]	-	-	-		
Momentum	[128, 521, 2048]	[1e-5, 1e-2]	[1e-6, 1e-2]	[0, 0.99999]	-	-	[1e-1, 1e+5]	[1e+0, 1e+4]
Nesterov	[128, 521, 2048]	[1e-5, 1e-2]	[1e-6, 1e-2]	[0, 0.99999]	-	-	[1e-1, 1e+5]	[1e+0, 1e+4]
RMSprop	[128, 521, 2048]	[1e-5, 1e-2]	[1e-6, 1e-2]	[0, 0.99999]	[0, 0.999]	[1e-8, 1e-3]	[1e-1, 1e+5]	[1e+0, 1e+4]

	B	η	λ	β_1	β_2	ϵ	λ_{IRM}	N_{IRM}
Adam	[128, 521, 2048]	[1e-5, 1e-2]	-	[0, 0.999]	[0, 0.999]	[1e-8, 1e-3]	[1e-1, 1e+5]	[1e+0, 1e+4]

E.2 Backgrounds Challenge Dataset

We conduct Bayesian optimization for the Backgrounds Challenge dataset as well. We use 4096 as the batch size. For all configurations other than batch size, as we follow Choi et al. (2019).

We conduct the hyperparameter search and restart training from scratch. Of the trained models, we evaluate trained model performance in the OOD dataset.

Table 8: Backgrounds Challenge: ResNet-50

	η	λ	γ
Momentum	[1e-5, 1e-2]	[1e-6, 1e-2]	[0, 0.99999]

	η	λ	β_1	β_2	ϵ
Adam	[1e-5, 1e-2]	[1e-6, 1e-2]	[0, 0.999]	[0, 0.999]	[1e-8, 1e-3]

E.3 WILDS

We conduct Bayesian optimization for the hyperparameter search of WILDS. The hyperparameters are sampled by uniform distribution whose minimum and maximum values are shown in the table 9 and 10. Note that the values for batch size B is fixed in these experiments due to computational efficiency. We implement IRMv1 as well as DomainBed experiments.

For training the Amazon-WILDS and CivilComments-WILDS datasets that we used as NLP datasets, we followed the deep neural network model and training configuration proposed in the original paper. DistilBERT, a distillation of BERT Base, is used as the deep neural network model.

Table 9: WILDS-Amazon: DistilBERT

	B	η	λ	γ	α	ϵ	λ_{IRM}	N_{IRM}
SGD	[8]	[1e-5, 1e-2]	[1e-6, 1e-2]	-	-	-	[1e-1, 1e+5]	[1e+0, 1e+4]
Momentum	[8]	[1e-5, 1e-2]	[1e-6, 1e-2]	[0, 0.99999]	-	-	[1e-1, 1e+5]	[1e+0, 1e+4]
Nesterov	[8]	[1e-5, 1e-2]	[1e-6, 1e-2]	[0, 0.99999]	-	-	[1e-1, 1e+5]	[1e+0, 1e+4]
RMSprop	[8]	[1e-5, 1e-2]	[1e-6, 1e-2]	[0, 0.99999]	[0, 0.999]	[1e-8, 1e-3]	[1e-1, 1e+5]	[1e+0, 1e+4]

	B	η	λ	β_1	β_2	ϵ	λ_{IRM}	N_{IRM}
Adam	[8]	[1e-5, 1e-2]	[1e-6, 1e-2]	[0, 0.999]	[0, 0.999]	[1e-8, 1e-3]	[1e-1, 1e+5]	[1e+0, 1e+4]

	B	η	β_1	β_2	ϵ
AdamW	[8]	[1e-5, 1e-2]	[0.9]	[0.999]	[1e-8]

	B	η	γ	ϵ	ρ
SAM	[8]	[1e-5, 1e-2]	[0.9]	[1e-4]	[5e-2]

Table 10: WILDS-CivilComments: DistilBERT

	B	η	λ	γ	α	ϵ	λ_{IRM}	N_{IRM}
SGD	[16]	[1e-5, 1e-2]	[1e-6, 1e-2]	-	-	-	[1e-1, 1e+5]	[1e+0, 1e+4]
Momentum	[16]	[1e-5, 1e-2]	[1e-6, 1e-2]	[0, 0.99999]	-	-	[1e-1, 1e+5]	[1e+0, 1e+4]
Nesterov	[16]	[1e-5, 1e-2]	[1e-6, 1e-2]	[0, 0.99999]	-	-	[1e-1, 1e+5]	[1e+0, 1e+4]
RMSprop	[16]	[1e-5, 1e-2]	[1e-6, 1e-2]	[0, 0.99999]	[0, 0.999]	[1e-8, 1e-3]	[1e-1, 1e+5]	[1e+0, 1e+4]

	B	η	λ	β_1	β_2	ϵ	λ_{IRM}	N_{IRM}
Adam	[16]	[1e-5, 1e-2]	[1e-6, 1e-2]	[0, 0.999]	[0, 0.999]	[1e-8, 1e-3]	[1e-1, 1e+5]	[1e+0, 1e+4]

E.4 CIFAR10-C and CIFAR10-P

Corruption: The corruption dataset we consider contains 19 corruption patterns. These are *Gaussian Noise*, *Shot Noise*, *Impulse Noise*, *Defocus Blur*, *Frosted Glass Blur*, *Motion Blur*, *Zoom Blue*, *Show*, *Frost*, *Fog*, *Brightness*, *Contrast*, *Elastic*, *Pixelate*, and *JPEG*. Sample corrupted images are shown in the original paper by Hendrycks & Dietterich (2019). Following Hendrycks & Dietterich (2019), we compute the classification error $E_{s,c}$ for each corruption c with a five-point scale for the noise severity s. Averaging over a five-point scale, we measure the classification accuracy for each corruption Acc_c as follows:

$$\text{Acc}_c = 1 - \frac{\sum_{s=1}^{5} E_{s,c}}{5} \tag{15}$$

This accuracy is the test accuracy (corruption) we defined in the main body of this paper. We evaluate the generalization performance by comparing this quantity with the accuracy calculated using the original test dataset $\text{Acc} = 1 - E$. Note that E is the classification error for the test (training domain) samples.

Perturbation: The perturbation dataset has six corruption patterns that are the same as in the corruption dataset and four additional digital transformations: *Gaussian Noise*, *Shot Noise*, *Motion Blur*, *Zoom Blur*, *Show*, *Brightness*, *Translate*, *Rotate*, *Tilt*, and *Scale*. The perturbation dataset differs from the corruption dataset in that each corruption generates more than thirty perturbation sequences. Hence, we use not a simple measure of accuracy but the following metric to determine the perturbation robustness:

$$d\left(\tau(\boldsymbol{x}), \tau\left(\boldsymbol{x}'\right)\right) = \sum_{i=1}^{5} \sum_{j=\min\{i,\sigma(i)\}+1}^{\max\{i,\sigma(i)\}} \mathbf{1}(1 \leq j-1 \leq 5), \tag{16}$$

where $\tau(\boldsymbol{x})$ is the ranked prediction of the classifier on image $\boldsymbol{x}$ and $\sigma(i) = \tau(\boldsymbol{x}')/\tau(\boldsymbol{x})$. This criterion measures how the top-5 prediction on two different images differs. By using this quantity, top-5 robustness perturbation can be written as follows:

$$\text{uT5D}_p = \frac{1}{m(n-1)} \sum_{i=1}^{m} \sum_{j=2}^{n} d\left(\tau\left(\boldsymbol{x}_j\right), \tau\left(\boldsymbol{x}_{j-1}\right)\right). \tag{17}$$

Table 11: Hyperparameter Search Range: ResNet-8 / CIFAR10

	B	η	λ	γ
Momentum	256	[1e-6, 1e+1]	[1e-5, 1e-4]	[1e-4 0.9999]

	B	η	λ	β_1	β_2	ϵ
Adam	256	[1e-4, 1e-1]	[1e-5, 1e-4]	[0.9, 0.999]	[0.99, 0.9999]	[1e-4, 1e-2]

F Full Results of Experiments

We conducted an evaluation of optimizers using two distinct model selection strategies. One approach is Oracle-based, while the other employs a method of training-domain validation set (Gulrajani & Lopez-Paz, 2021). In Section F.1, we compare the OOD accuracy of models obtained through each strategy, as displayed in a tabular format. Particularly for the latter strategy, we present both the average and variance of the Top-10 models, as well as the average and variance for models surpassing a certain threshold.

The rationale behind providing the average and variance of the Top-10 models lies in our adoption of Bayesian optimization for hyperparameters, with the aim of illustrating the error bars of high-performing models obtained through this method. The results for models exceeding a certain threshold (in the rightmost bin) are shared to facilitate comparison of average OOD accuracy performance when non-adaptive and adaptive optimization methods are comparable in terms of ID accuracy.

In Section F.2, we present the results for all hyperparameters we explored (except for the model inferior to random guess), along with their distributions in a box plot. Finally, in Section F.4, we present the OOD accuracy and ID accuracy results for all the results from which these results are derived as a scatter plot.

F.1 Full Results of Table

Oracle:
In this section, we provide additional information on Table 1 in the paper. Table 12 shows the mean and standard deviation for the top-10 models, including those selected by the Oracle model selection method. In eight of the ten datasets, the non-adaptive method outperforms the adaptive method in out-of-distribution accuracy.

Table 12: Top-10 Trials: Mean and Standard Deviation for Each Dataset (Model Selection by Oracle). The variance is relatively suppressed in many tasks because it is the mean and variance of the model that achieves Top-10 OOD accuracy.

Model	OOD Dataset	Non-Adaptive Optimizer			Adaptive Optimizer	
		SGD	Momentum	Netsterov	RMSProp	Adam
4-Layer CNN	RotatedMNIST	$89.62_{\pm 0.18}$	$93.23_{\pm 0.69}$	$92.89_{\pm 0.2}$	$95.81_{\pm 0.16}$	$\mathbf{96.05_{\pm 0.16}}$
	ColoredMNIST	$14.64_{\pm 0.07}$	$29.80_{\pm 1.84}$	$28.85_{\pm 2.0}$	$\mathbf{52.82_{\pm 6.21}}$	$52.39_{\pm 6.89}$
ResNet50	VLCS	$\mathbf{98.98_{\pm 0.1}}$	$98.70_{\pm 0.16}$	$98.49_{\pm 0.12}$	$96.23_{\pm 1.39}$	$97.09_{\pm 1.61}$
	PACS	$86.56_{\pm 0.83}$	$\mathbf{86.90_{\pm 0.82}}$	$86.01_{\pm 1.36}$	$81.10_{\pm 2.93}$	$82.59_{\pm 2.93}$
	OfficeHome	$63.68_{\pm 0.12}$	$\mathbf{63.52_{\pm 0.44}}$	$62.40_{\pm 0.47}$	$55.34_{\pm 3.39}$	$62.12_{\pm 0.35}$
	TerraIncognita	$52.22_{\pm 1.62}$	$\mathbf{56.05_{\pm 1.96}}$	$52.98_{\pm 1.61}$	$53.67_{\pm 2.62}$	$48.78_{\pm 3.53}$
	DomainNet	$55.31_{\pm 2.38}$	$56.12_{\pm 3.85}$	$\mathbf{58.19_{\pm 2.2}}$	$52.71_{\pm 2.74}$	$55.74_{\pm 1.65}$
	BackgroundChallenge	-	$\mathbf{78.99_{\pm 0.48}}$	-	-	$75.55_{\pm 1.5}$
DistilBERT	WILDS_amazon	$52.00_{\pm 0.0}$	$\mathbf{54.67_{\pm 0.0}}$	$\mathbf{54.67_{\pm 0.0}}$	$48.67_{\pm 3.46}$	$52.44_{\pm 1.5}$
	WILDS_civilcomments	$51.81_{\pm 0.29}$	$\mathbf{56.40_{\pm 0.61}}$	$55.98_{\pm 0.47}$	$38.42_{\pm 7.04}$	$37.71_{\pm 4.0}$
ResNet-20	ColoredMNIST	-	$28.93_{\pm 2.63}$	-	-	$\mathbf{29.84_{\pm 1.64}}$
ViT	PACS	-	$\mathbf{90.28_{\pm 0.54}}$	-	-	$90.05_{\pm 0.29}$

Training-Domain Validation Set: Table 13 shows the results of top-10 models with training-domain validation set (Gulrajani & Lopez-Paz, 2021) as the model selection method. It shows that 11 out of 12 tasks showed that the non-adaptive optimization method is superior. As exhibited in Table 14, we present the out-of-distribution accuracy along with the mean and standard deviation of the subset exhibiting high

validation performance within our targeted training domain, as graphically depicted in Figure 1. This data specifically corresponds to the apex of the rightmost bin in the bar chart encapsulated in Figure 1. As noted, the relatively elevated standard deviations observed can be primarily attributed to our calculation methodology. This approach calculates the mean and standard deviation values of the out-of-distribution accuracy, specifically focusing on the rightmost bins indicative of high validation accuracy as portrayed in Figure 1. It is crucial to acknowledge that this unique approach could potentially yield a broader range of variances.

Table 13: Top-10 Trials: Mean and Standard Deviation for Each Dataset (Model Selection by Training-Domain Validation Set). The variance is relatively suppressed in many tasks because it is the mean and variance of the model that achieves Top-10 OOD accuracy.

Model	OOD Dataset	Non-Adaptive Optimizer			Adaptive Optimizer	
		SGD	Momentum	Netsterov	RMSProp	Adam
4-Layer CNN	RotatedMNIST	89.13$_{\pm 0.56}$	93.09$_{\pm 0.82}$	91.36$_{\pm 1.4}$	95.51$_{\pm 0.48}$	**95.76$_{\pm 0.43}$**
	ColoredMNIST	10.4$_{\pm 0.3}$	10.04$_{\pm 0.07}$	**10.09$_{\pm 0.44}$**	9.84$_{\pm 0.18}$	10.08$_{\pm 0.4}$
ResNet50	VLCS	**98.32$_{\pm 0.34}$**	98.15$_{\pm 0.57}$	97.93$_{\pm 0.28}$	94.49$_{\pm 3.9}$	96.76$_{\pm 2.56}$
	PACS	85.01$_{\pm 1.27}$	**85.60$_{\pm 1.21}$**	84.91$_{\pm 1.53}$	81.10$_{\pm 2.93}$	82.36$_{\pm 3.11}$
	OfficeHome	62.62$_{\pm 0.74}$	**62.65$_{\pm 1.02}$**	60.98$_{\pm 1.46}$	55.02$_{\pm 3.94}$	60.09$_{\pm 1.08}$
	TerraIncognita	**46.84$_{\pm 4.15}$**	44.67$_{\pm 9.2}$	45.21$_{\pm 4.88}$	44.48$_{\pm 7.96}$	41.82$_{\pm 7.65}$
	DomainNet	55.25$_{\pm 2.51}$	55.96$_{\pm 4.1}$	**58.19$_{\pm 2.2}$**	52.71$_{\pm 2.74}$	55.67$_{\pm 1.78}$
	BackgroundChallenge	-	**78.99$_{\pm 0.48}$**	-	-	75.55$_{\pm 1.5}$
DistilBERT	WILDS_amazon	52.00$_{\pm 0.0}$	**54.13$_{\pm 0.69}$**	53.77$_{\pm 0.63}$	50.93$_{\pm 3.25}$	52.44$_{\pm 1.5}$
	WILDS_civilcomments	49.17$_{\pm 1.09}$	50.09$_{\pm 1.91}$	**50.40$_{\pm 1.54}$**	31.65$_{\pm 12.56}$	33.13$_{\pm 5.89}$
ResNet-20	ColoredMNIST	-	**11.00$_{\pm 0.52}$**	-	-	10.09$_{\pm 0.15}$
ViT	PACS	-	**90.28$_{\pm 0.54}$**	-	-	90.05$_{\pm 0.29}$

Table 14: Trials in Rightmost Bin: Mean and Standard Deviation for Each Dataset (Model Selection by Training-Domain Validation Set). The variance is relatively large because we compute the mean and variance of models that exceed a specific threshold (the rightmost bin in Figure 1) in ID accuracy.

Model	OOD Dataset	Non-Adaptive Optimizer			Adaptive Optimizer	
		SGD	Momentum	Netsterov	RMSProp	Adam
4-Layer CNN	RotatedMNIST	82.83$_{\pm 6.15}$	87.84$_{\pm 5.27}$	87.43$_{\pm 5.58}$	94.29$_{\pm 1.22}$	**94.43**$_{\pm 1.91}$
	ColoredMNIST	10.93$_{\pm 1.61}$	12.86$_{\pm 4.66}$	10.44$_{\pm 2.53}$	**22.84**$_{\pm 6.45}$	16.12$_{\pm 7.98}$
ResNet50	VLCS	**97.95**$_{\pm 1.02}$	96.81$_{\pm 2.96}$	96.54$_{\pm 2.38}$	94.07$_{\pm 3.4}$	94.49$_{\pm 6.59}$
	PACS	**79.67**$_{\pm 4.35}$	78.58$_{\pm 6.07}$	78.11$_{\pm 5.9}$	74.98$_{\pm 8.59}$	70.86$_{\pm 6.96}$
	OfficeHome	**61.11**$_{\pm 2.07}$	60.38$_{\pm 2.35}$	58.29$_{\pm 2.58}$	55.98$_{\pm 3.39}$	57.74$_{\pm 3.1}$
	TerraIncognita	**42.56**$_{\pm 5.31}$	42.22$_{\pm 8.33}$	41.44$_{\pm 6.3}$	41.96$_{\pm 10.36}$	40.76$_{\pm 8.06}$
	DomainNet	55.79$_{\pm 1.94}$	57.40$_{\pm 3.1}$	**57.51**$_{\pm 2.55}$	55.09$_{\pm 0.65}$	56.05$_{\pm 1.41}$
	BackgroundChallenge	-	**74.98**$_{\pm 4.7}$	-	-	69.14$_{\pm 5.61}$
DistilBERT	Amazon-WILDS	50.58$_{\pm 1.07}$	**52.20**$_{\pm 1.49}$	52.00$_{\pm 1.56}$	51.73$_{\pm 1.55}$	51.32$_{\pm 1.83}$
	CivilComments-WILDS	42.24$_{\pm 5.8}$	**44.79**$_{\pm 6.57}$	44.15$_{\pm 6.37}$	21.79$_{\pm 9.59}$	23.55$_{\pm 7.43}$
ResNet-20	ColoredMNIST	-	19.62$_{\pm 7.35}$	-	-	**21.70$_{\pm 7.66}$**
ViT	PACS	-	**87.07$_{\pm 5.52}$**	-	-	85.17$_{\pm 7.67}$

F.2 Full Results of Boxplot

Since we could not include all the results in the main paper, we report all the OOD accuracy, ID accuracy and their difference (we denote as gap) results including ERM and IRM results in a box plot.

F.2.1 Full Results of Filtered Boxplot (ERM)

What we want to find out is the OOD generalization performance for models that perform better than random guess in the ID test set, i.e., models that have been trained. As Filtered Results, we define random guess = 1/num of classes in each problem setting, and show the results of eliminating those models whose ID accuracy does not exceed this threshold.

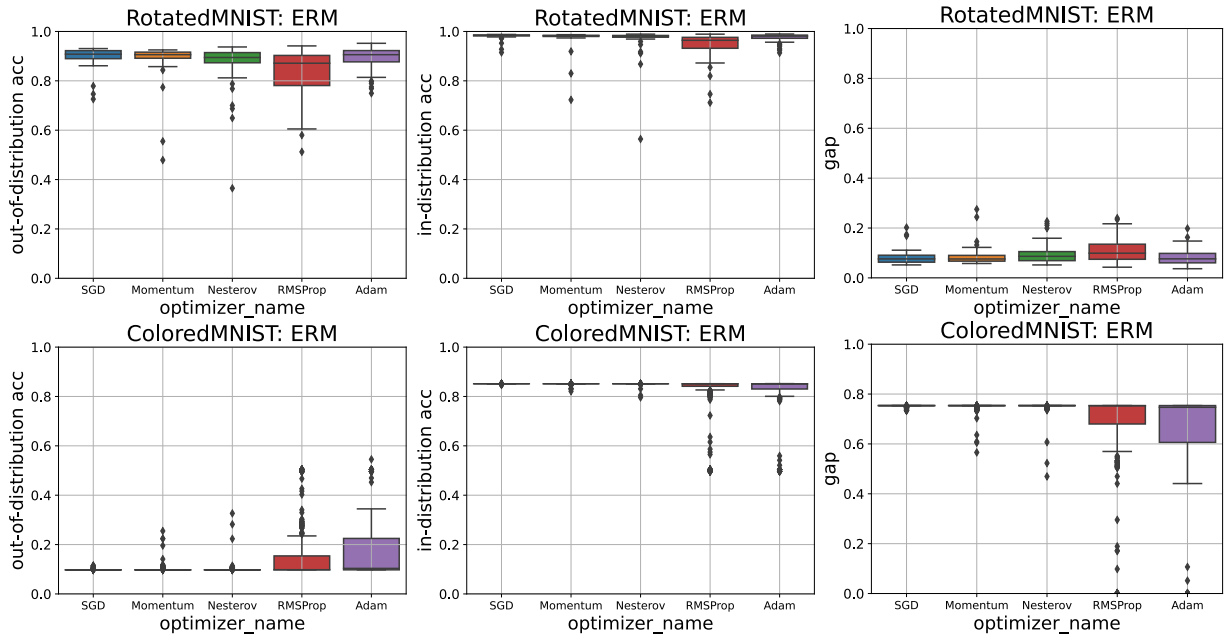

Figure 6. Filtered Results of RotatedMNIST and ColoredMNIST in DomainBed: Comparison of the in-distribution (validation) accuracy and the out-of-distribution (test) accuracy of ERM across five optimizers.

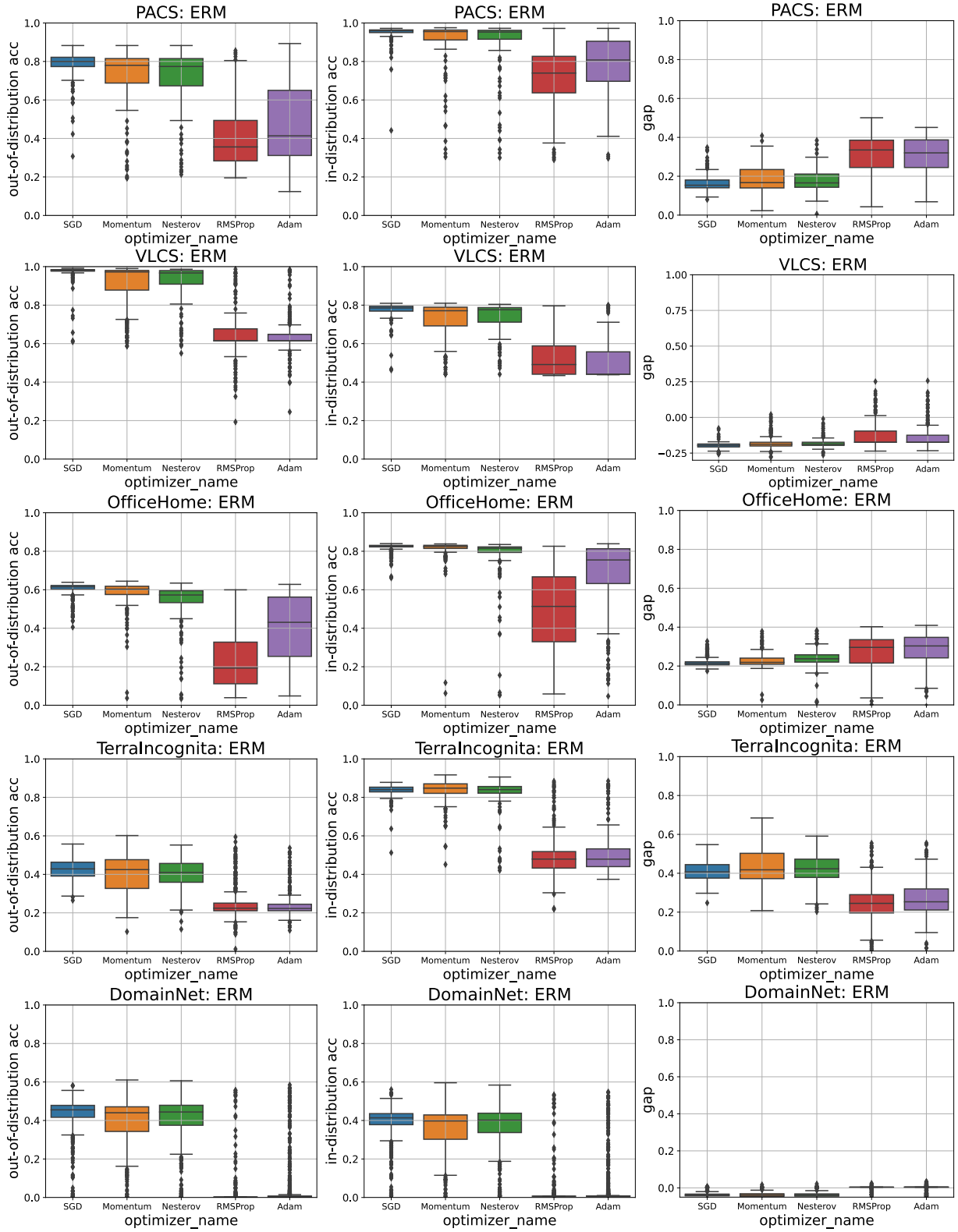

Figure 7. Filtered Results of PACS, VLCS, OfficeHome, TerraIncognita, and DomainNet in DomainBed: Comparison of the in-distribution (validation) accuracy and the out-of-distribution (test) accuracy of ERM across five optimizers.

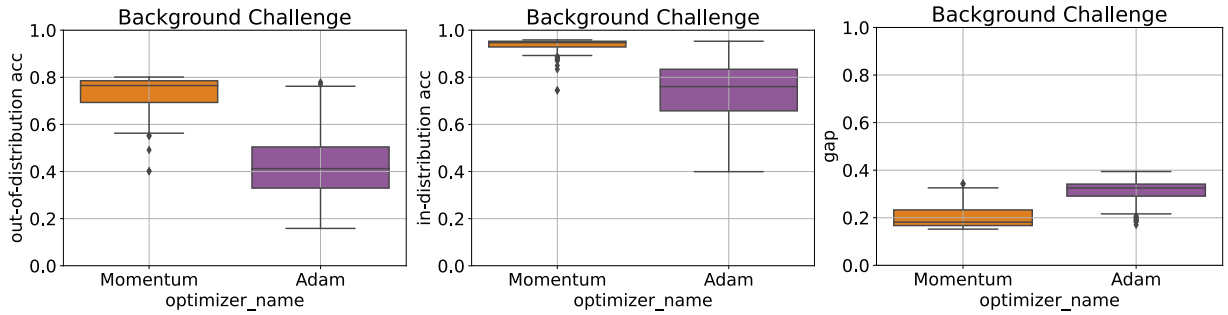

Figure 8. Filtered Results of Backgrounds Challenge: Comparison of the in-distribution (validation) accuracy and the out-of-distribution (test) accuracy of ERM across five optimizers.

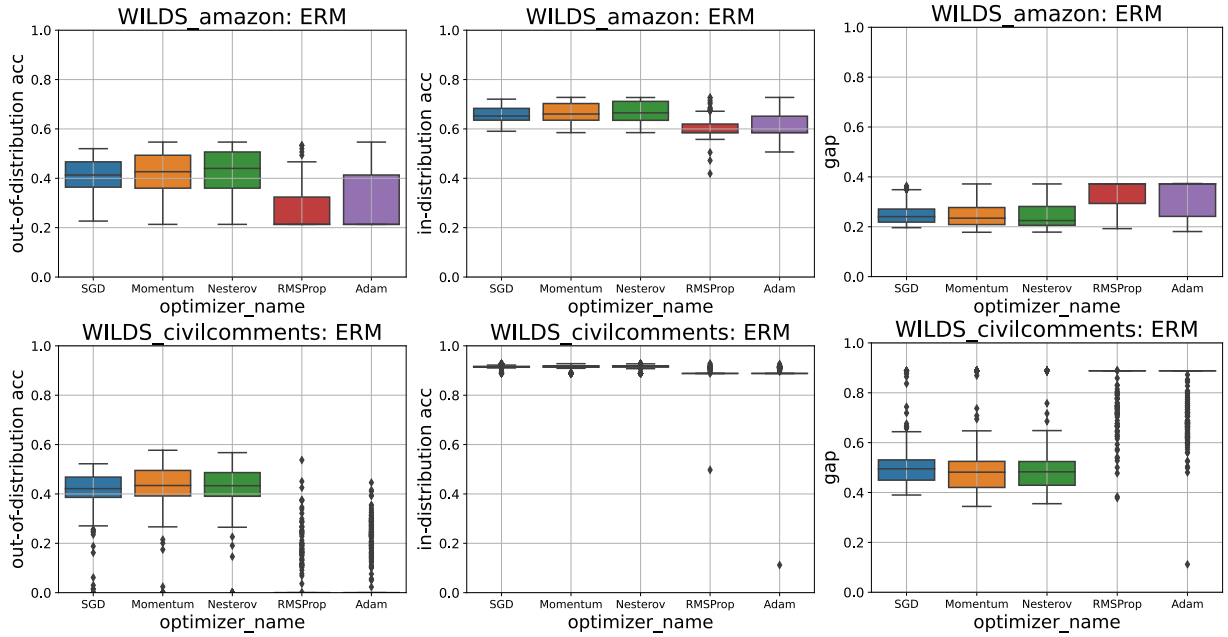

Figure 9. Filtered Results of Amazon-WILDS and CivilComments-WILDS: Comparison of the in-distribution (validation) accuracy and the out-of-distribution (test) accuracy of ERM across five optimizers.

F.2.2 Full Results of Filtered Boxplot (IRM)

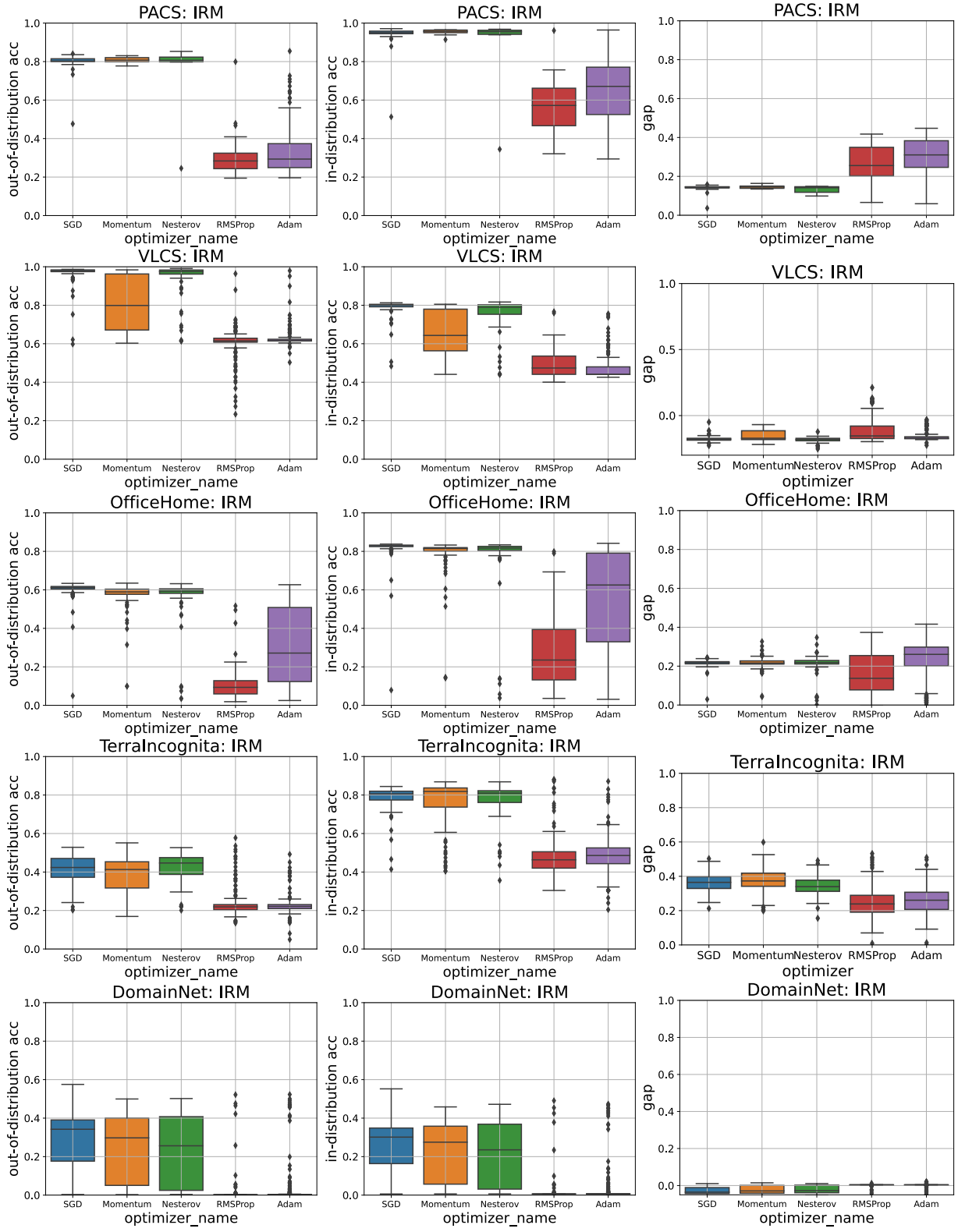

Figure 10. Filtered Results of PACS, VLCS, OfficeHome, TerraIncognita and DomainNet in DomainBed: Comparison of the in-distribution (validation) accuracy and the out-of-distribution (test) accuracy of IRM across five optimizers.

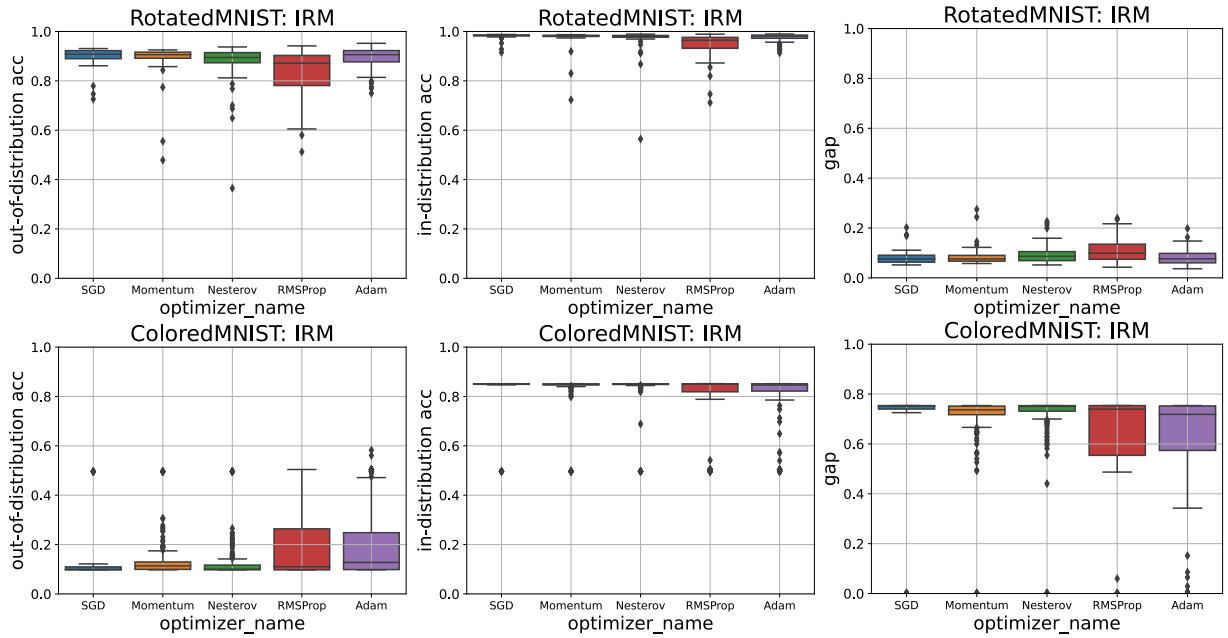

Figure 11. Filtered Results of RotatedMNIST and ColoredMNIST in DomainBed: Comparison of the in-distribution (validation) accuracy and the out-of-distribution (test) accuracy of IRM across five optimizers.

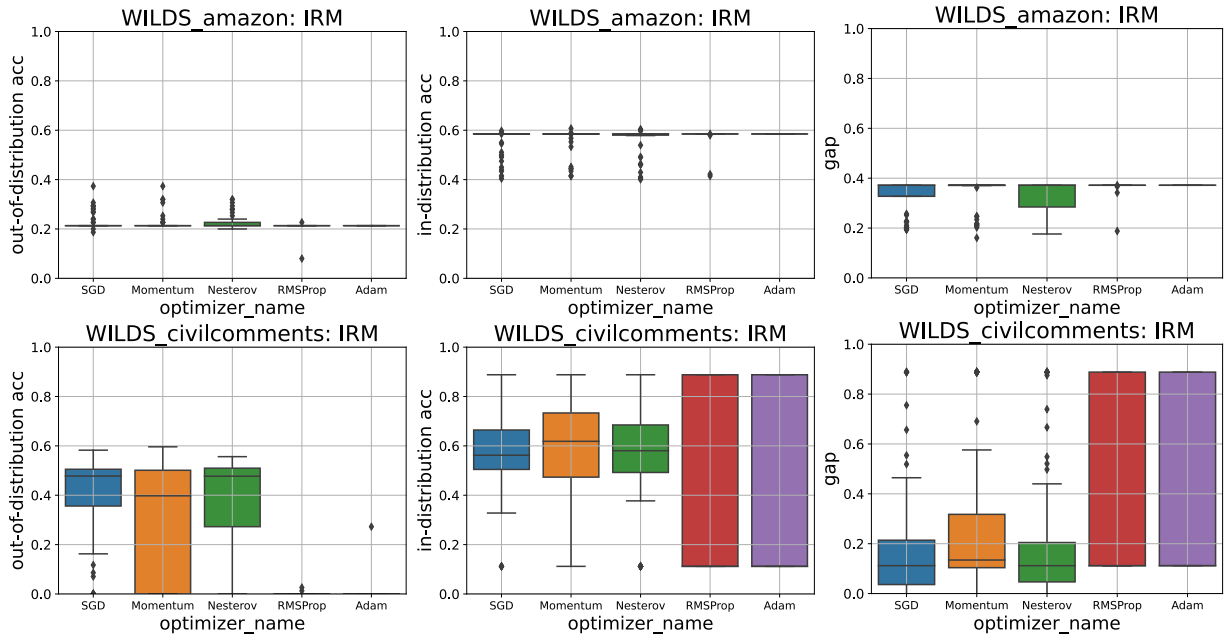

Figure 12. Filtered Results of Amazon-WILDS and CivilComments-WILDS: Comparison of the in-distribution (validation) accuracy and the out-of-distribution (test) accuracy of IRM across five optimizers.

F.3 Full Results of Bin-Diagram Plots

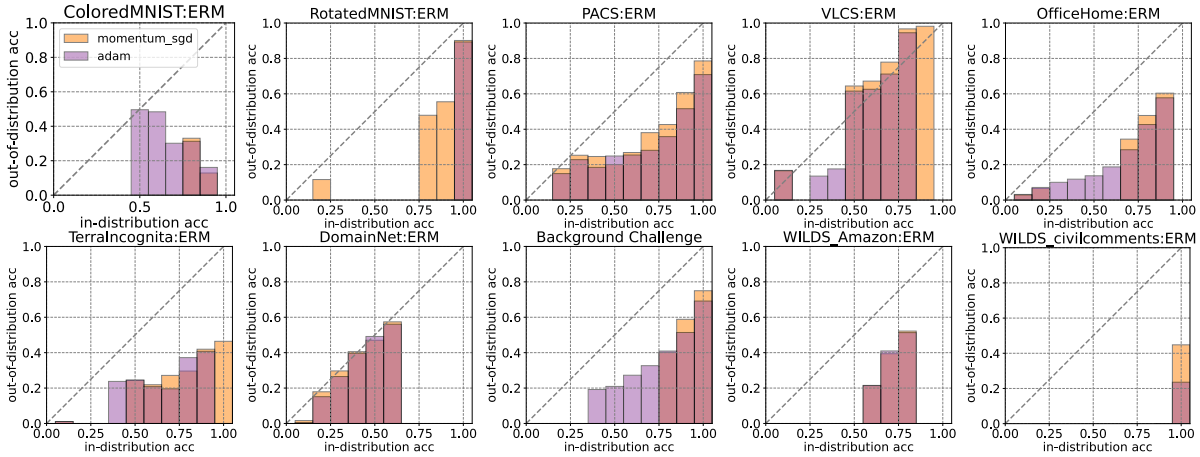

Figure 13. DomainBed, Backgrounds Challenge, Amazon-WILDS, and CivilComments-WILDS: Comparison of the in-distribution accuracy and the out-of-distribution accuracy of ERM between Momentum SGD and Adam. Since Adam showed better OOD performance than RMSProp, Adam is presented as a representative of adaptive methods. Momentum SGD shows competitive performance in OOD with Vanilla SGD and Nesterov Momentum and is a representative of non-adaptive methods.

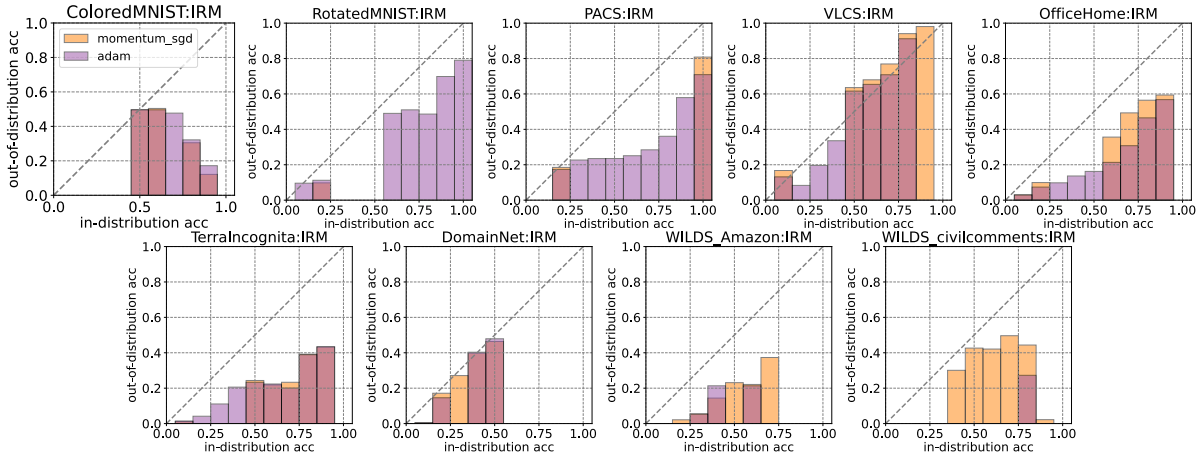

Figure 14. DomainBed, Amazon-WILDS, and CivilComments-WILDS: Comparison of the in-distribution accuracy and the out-of-distribution accuracy of IRM between Momentum SGD and Adam. Since Adam showed better OOD performance than RMSProp, Adam is presented as a representative of adaptive methods. Momentum SGD shows competitive performance in OOD with Vanilla SGD and Nesterov Momentum and is a representative of non-adaptive methods.

F.4 Full Results of Scatter Plots

The results of the comparison of OOD accuracy and in-distribution accuracy shown in Section 4.3 are shown below for all benchmarks.

The box plots shown in Section F.2 and the Reliability Diagram Like Plot shown in Section F.3 are based on the data shown in the Scatter Plot shown below.

F.4.1 ERM

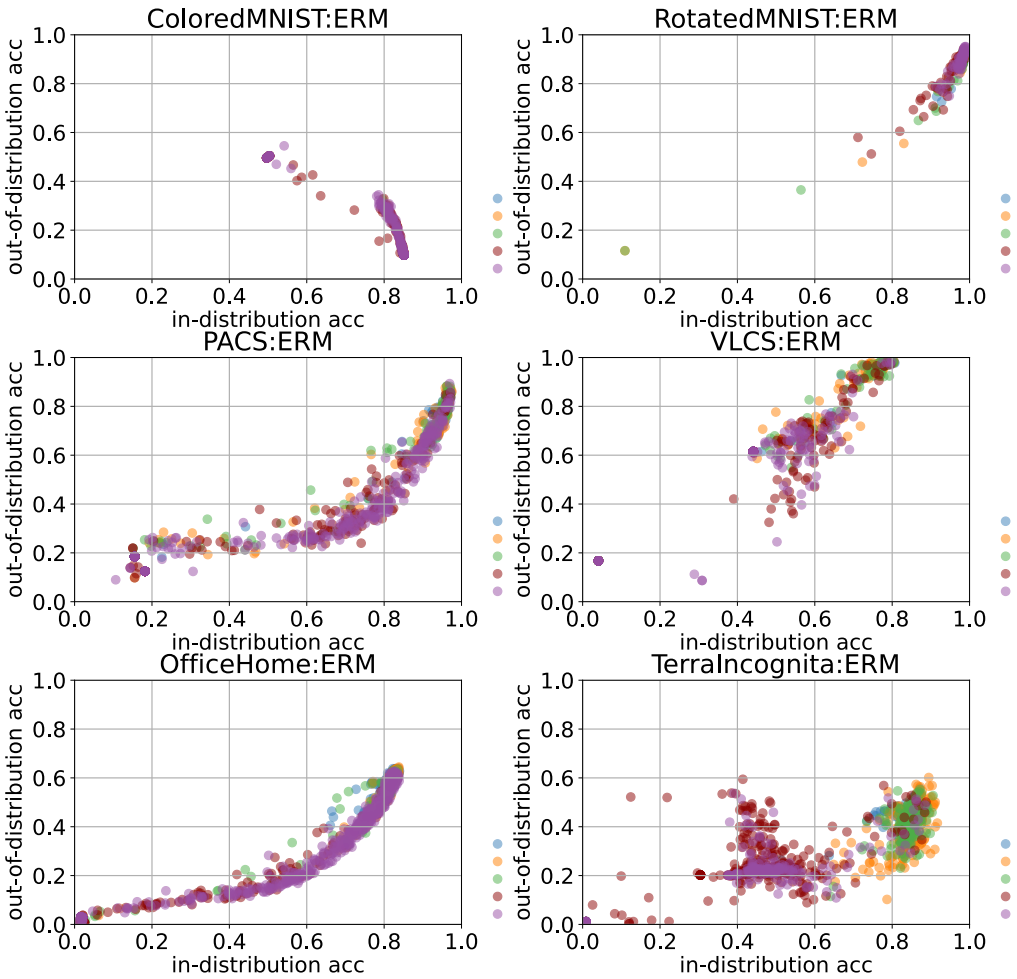

Figure 15. DomainBed (ColoredMNIST, RotatedMNIST, PACS, VLCS, OfficeHome and TerraIncognita): Comparison of the in-distribution accuracy and the out-of-distribution accuracy of ERM across optimizers. The legend circles on the right side of each figure show, in order, VanillaSGD, Momentum SGD, Nesterov Momentum, RMProp, and Adam. The difference in each data point indicates the difference in hyperparameter configuration.

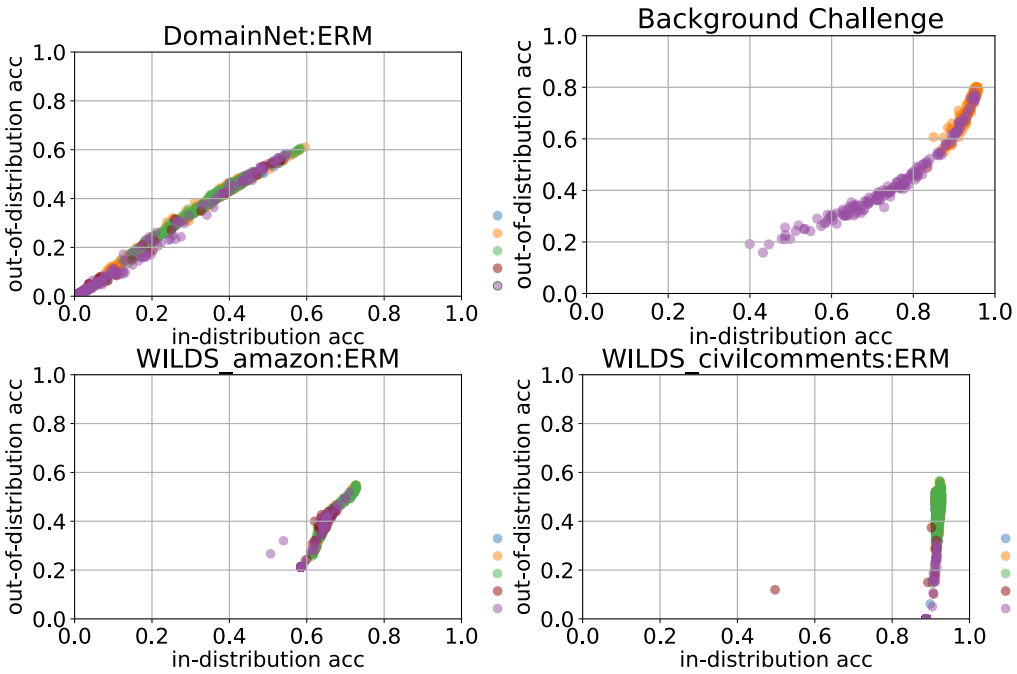

Figure 16. DomainBed (DomainNet), Backgrounds Challenge and WILDS: Comparison of the in-distribution accuracy and the out-of-distribution accuracy of ERM across optimizers. The legend circles on the right side of each figure show, in order, VanillaSGD, Momentum SGD, Nesterov Momentum, RMProp, and Adam. The difference in each data point indicates the difference in hyperparameter configuration.

F.4.2 IRM

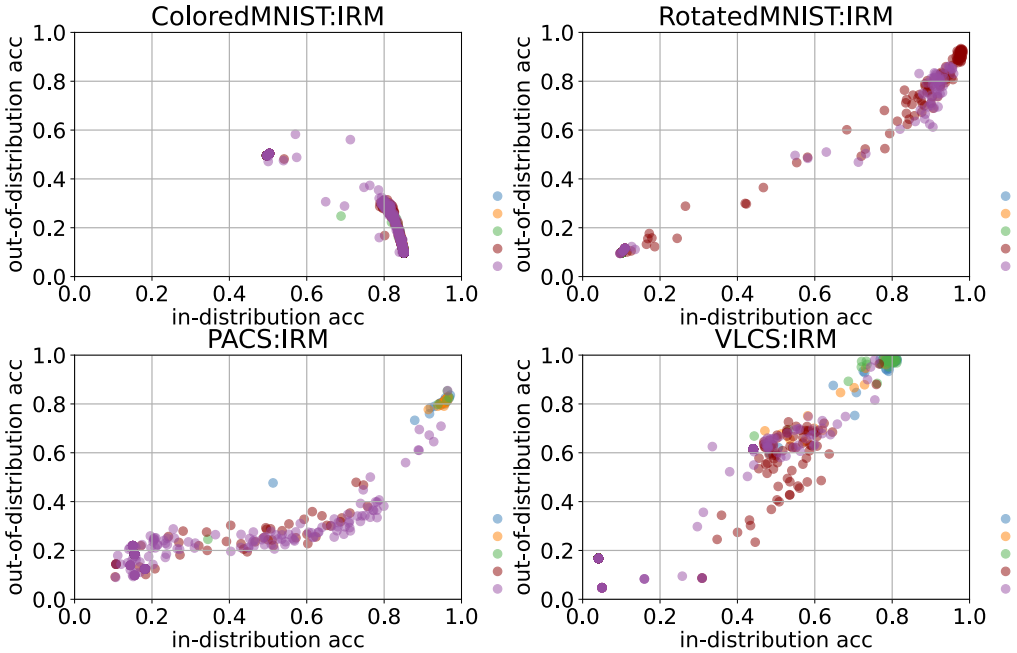

Figure 17. DomainBed (ColoredMNIST, RotatedMNIST, PACS and VLCS): Comparison of the in-distribution accuracy and the out-of-distribution accuracy of IRM across optimizers. The legend circles on the right side of each figure show, in order, VanillaSGD, Momentum SGD, Nesterov Momentum, RMProp, and Adam. The difference in each data point indicates the difference in hyperparameter configuration.

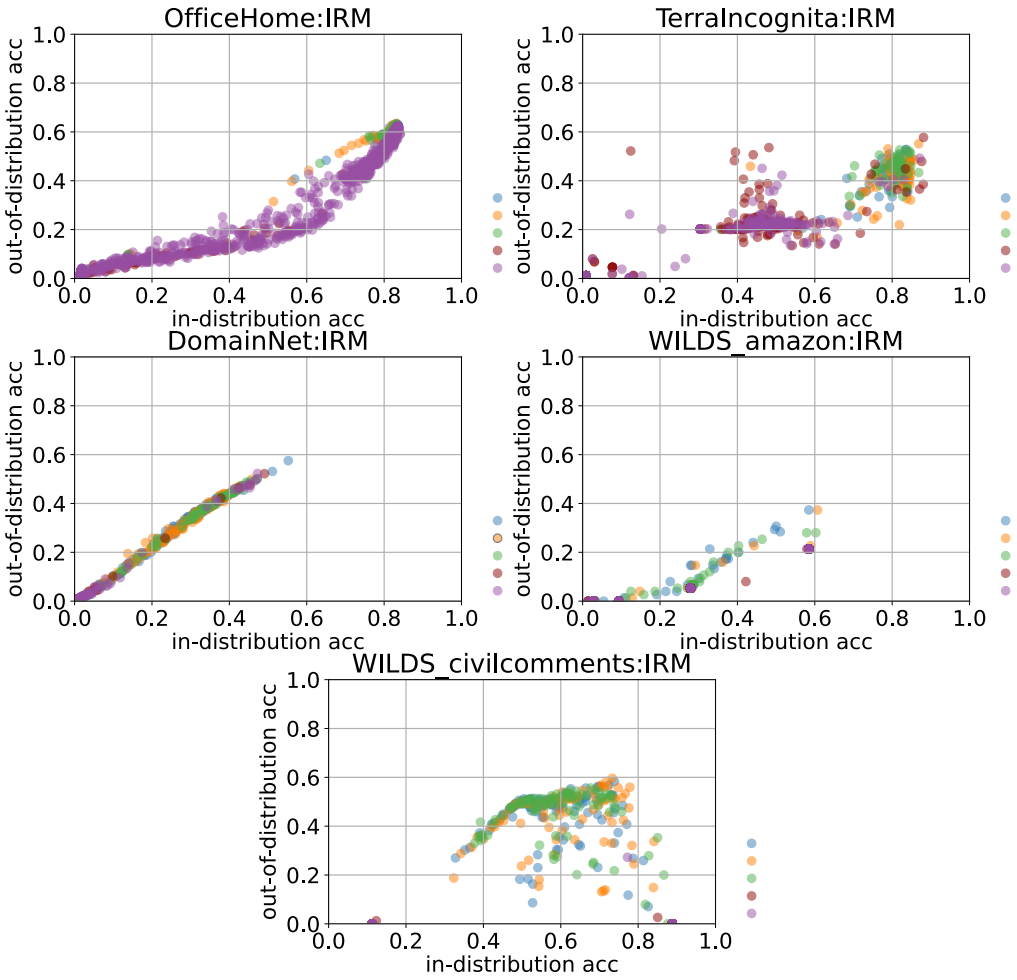

Figure 18. DomainBed (OfficeHome, TerraIncognita, DomainNet) and WILDS: Comparison of the in-distribution accuracy and the out-of-distribution accuracy of IRM across optimizers. The legend circles on the right side of each figure show, in order, VanillaSGD, Momentum SGD, Nesterov Momentum, RMProp, and Adam. The difference in each data point indicates the difference in hyperparameter configuration.

G Ablation Study

In addition to the experimental results presented in the main paper, we provide a more in-depth analysis, which is shown in this chapter.

First of all, We show that the pattern of linear correlation of accuracy claimed by (Miller et al., 2021) does not necessarily occur even when the correlation patterns we observed, such as diminishing returns, are probit transformed. The results of the probit transform of the scatter plots shown in Appendix F.4 are shown, following the method of (Miller et al., 2021). This may be due to the fact that our experimental setup uses a larger number of data sets and takes IRM and other factors into account.

In the second section, we present results comparing the performance improvement of OOD with a larger trial budget in the search for hyperparameters by Bayesian optimization.

Thirdly, We investigate why Adam shows better OOD performance than SGD in the negatively correlated case seen in Figure 6 for ColoredMNIST by considering the learning curve.

Finally, we examine the effectiveness of the early stopping for each optimizer to study if adaptive optimizers overfit because of their speed of convergence.

G.1 Probit Transformed Scatter Plot

As shown in Section 4.3, the work of (Miller et al., 2021) compares the accuracy of OOD with the accuracy of in-distribution by showing a plot on a probit scale. Their comparison shows that the correlation of accuracy is linear.

In this section, we convert the scatter plots identified in Section F.4 to probit scale and confirm that they do not necessarily show a linear correlation (Figure 19, 21, 22, 23, 23, and 24).

G.1.1 ERM

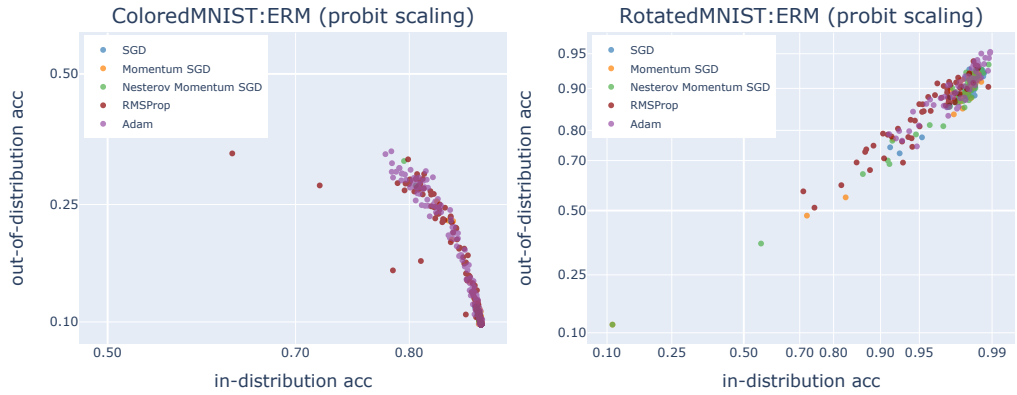

Figure 19. Probit Scale / DomainBed (ColoredMNIST and RotatedMNIST): Comparison of the in-distribution accuracy and the out-of-distribution accuracy of ERM across optimizers. The difference in each data point indicates the difference in hyperparameter configuration.

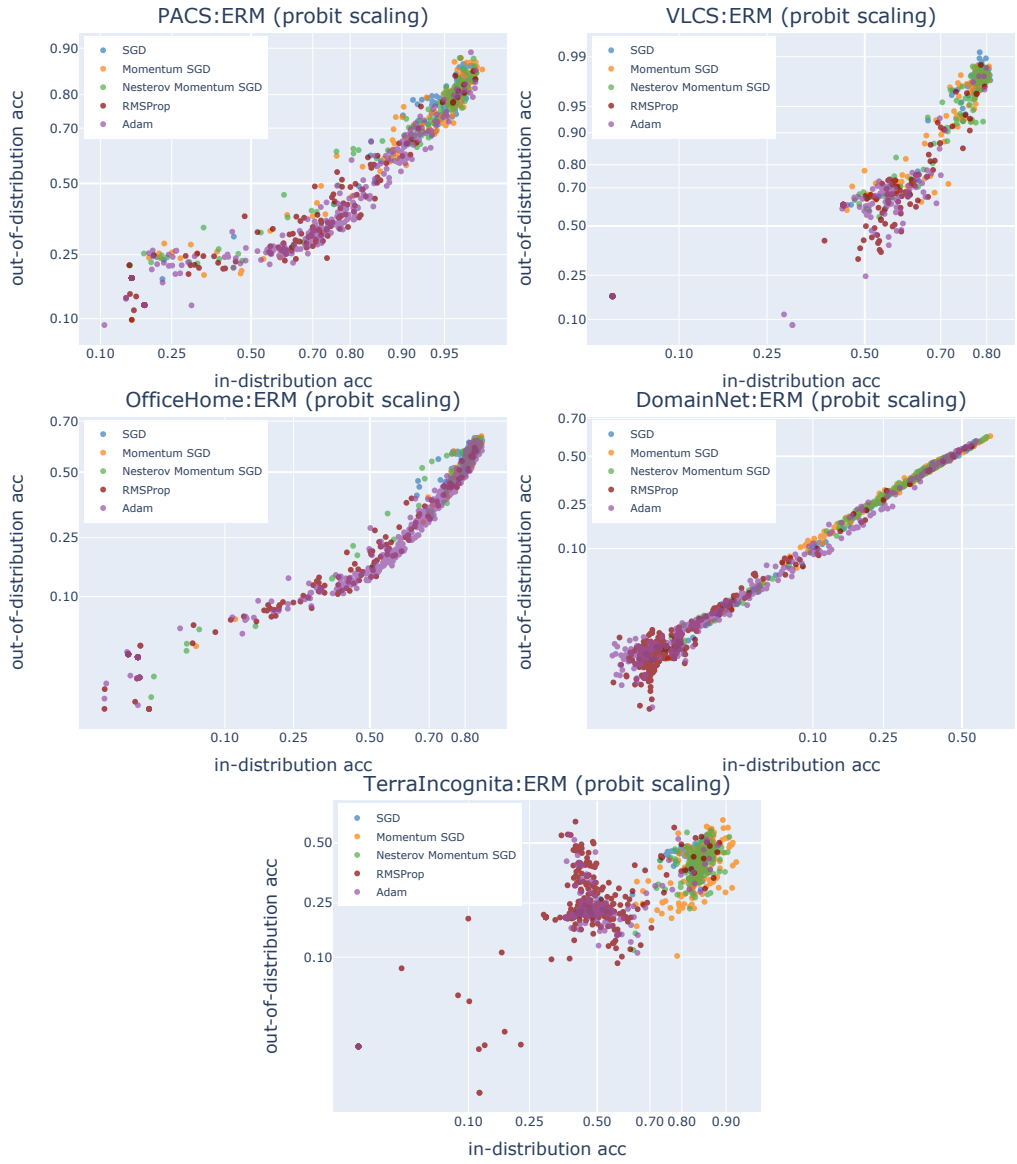

Figure 20. Probit Scale / DomainBed (PACS, VLCS, OfficeHome, DomainNet and TerraIncognita): Comparison of the in-distribution accuracy and the out-of-distribution accuracy of ERM across optimizers. The difference in each data point indicates the difference in hyperparameter configuration.

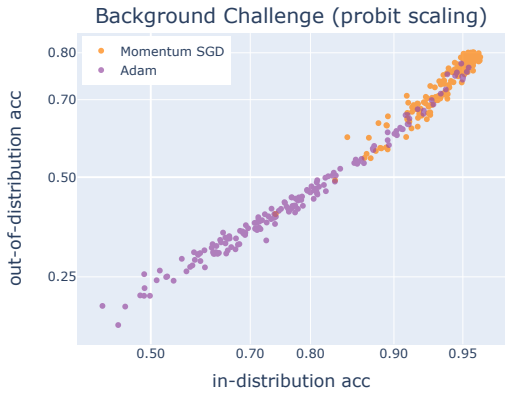

Figure 21. Probit Scale / Backgrounds Challenge: Comparison of the in-distribution accuracy and the out-of-distribution accuracy of ERM across optimizers. The difference in each data point indicates the difference in hyperparameter configuration.

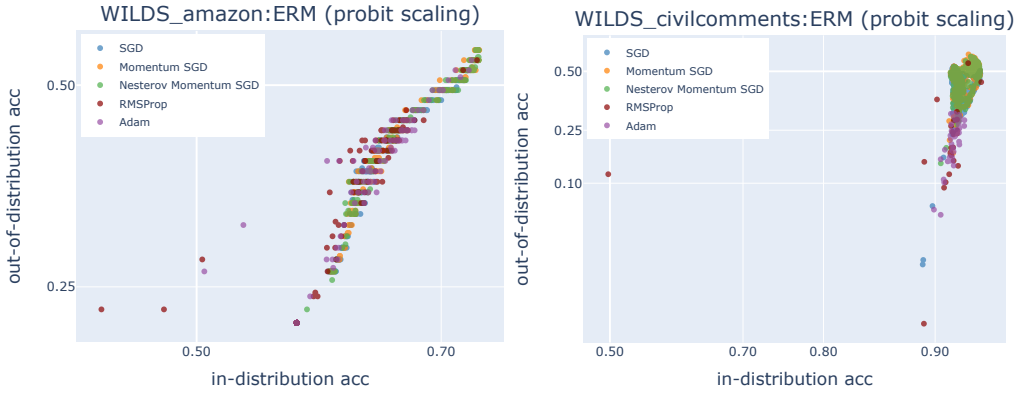

Figure 22. Probit Scale / WILDS: Comparison of the in-distribution accuracy and the out-of-distribution accuracy of ERM across optimizers. The difference in each data point indicates the difference in hyperparameter configuration.

G.1.2 IRM

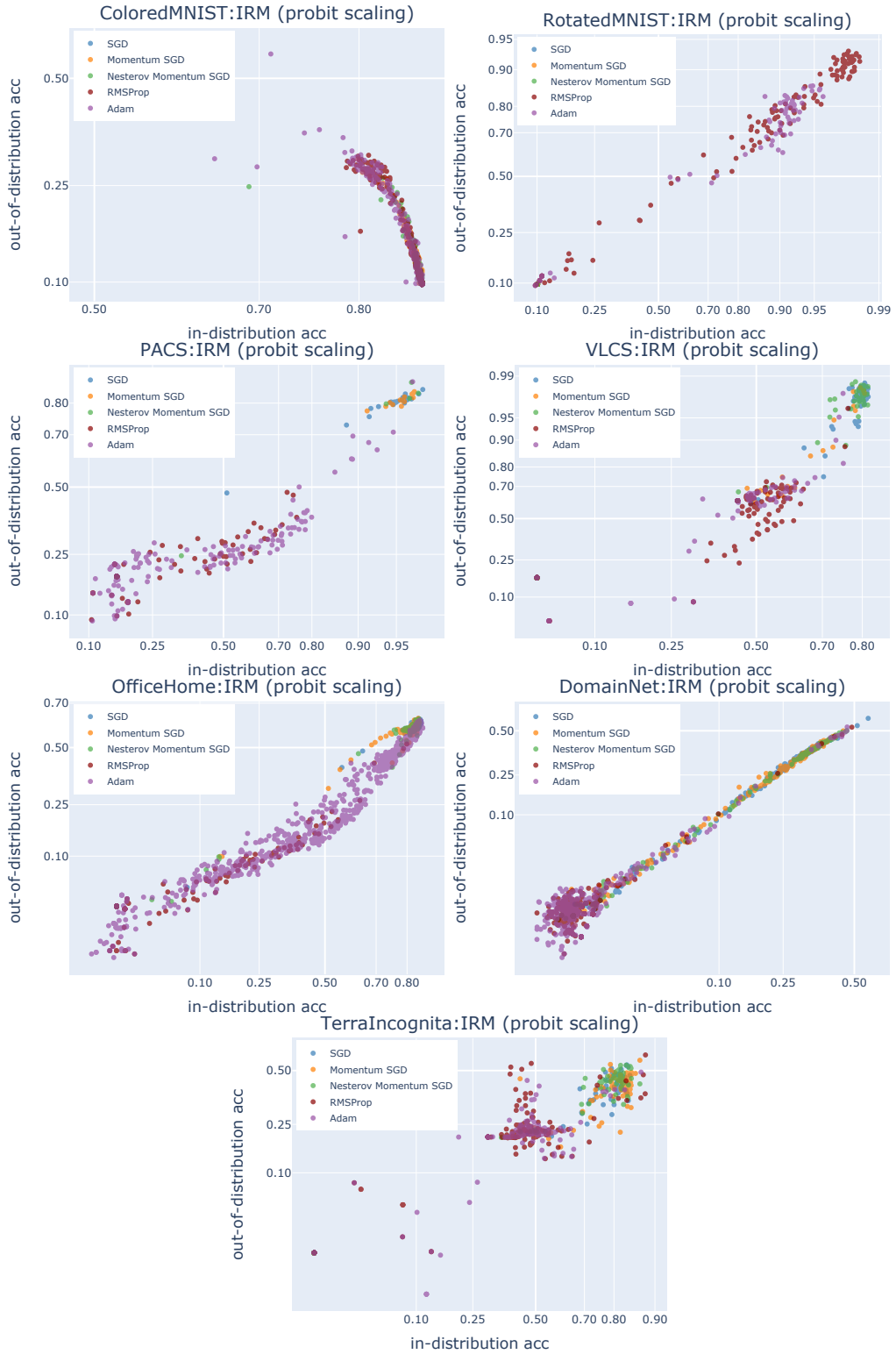

Figure 23. Probit Scale / DomainBed (ColoredMNIST, RotatedMNIST, PACS, VLCS, OfficeHome, DomainNed and TerraIncognita): Comparison of the in-distribution accuracy and the out-of-distribution accuracy of IRM across optimizers. The difference in each data point indicates the difference in hyperparameter configuration.

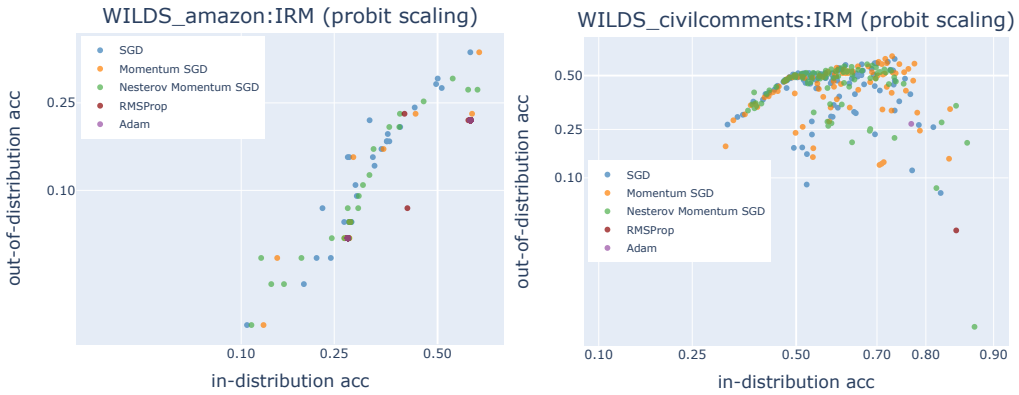

Figure 24. Probit Scale / WILDS: Comparison of the in-distribution accuracy and the out-of-distribution accuracy of IRM across optimizers. The difference in each data point indicates the difference in hyperparameter configuration.

G.2 Model Performance Transition throught Hyperparameter Search

For practitioners, we show how much the trial budget for hyperparameter optimization affects OOD generalization.

G.2.1 Hyperparameter Trial Budget vs OOD Accuracy

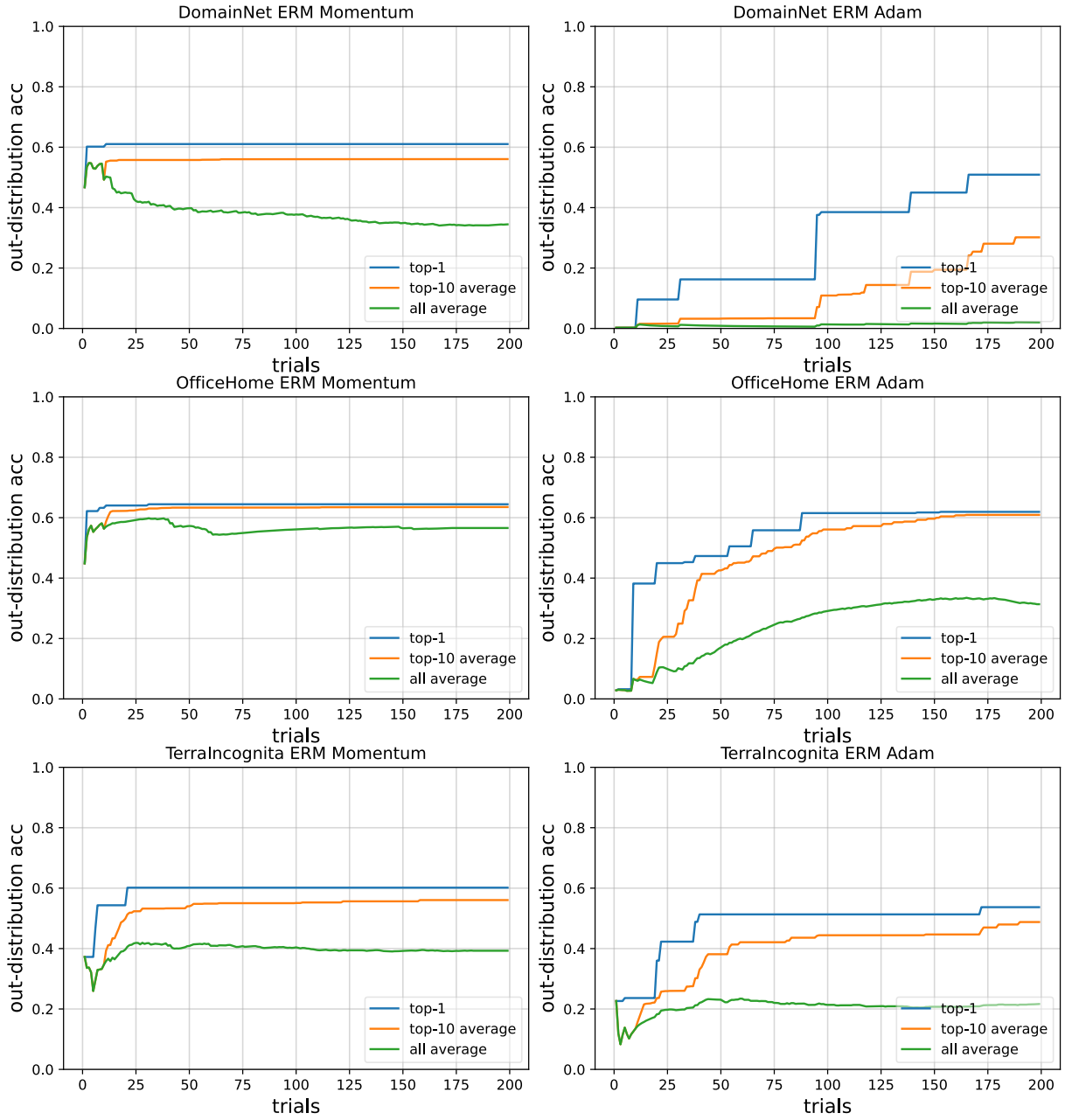

Figure 25. ERM DomainNet, OfficeHome and TerraIncognita / OOD accuracy when horizontal axis is the trial budget

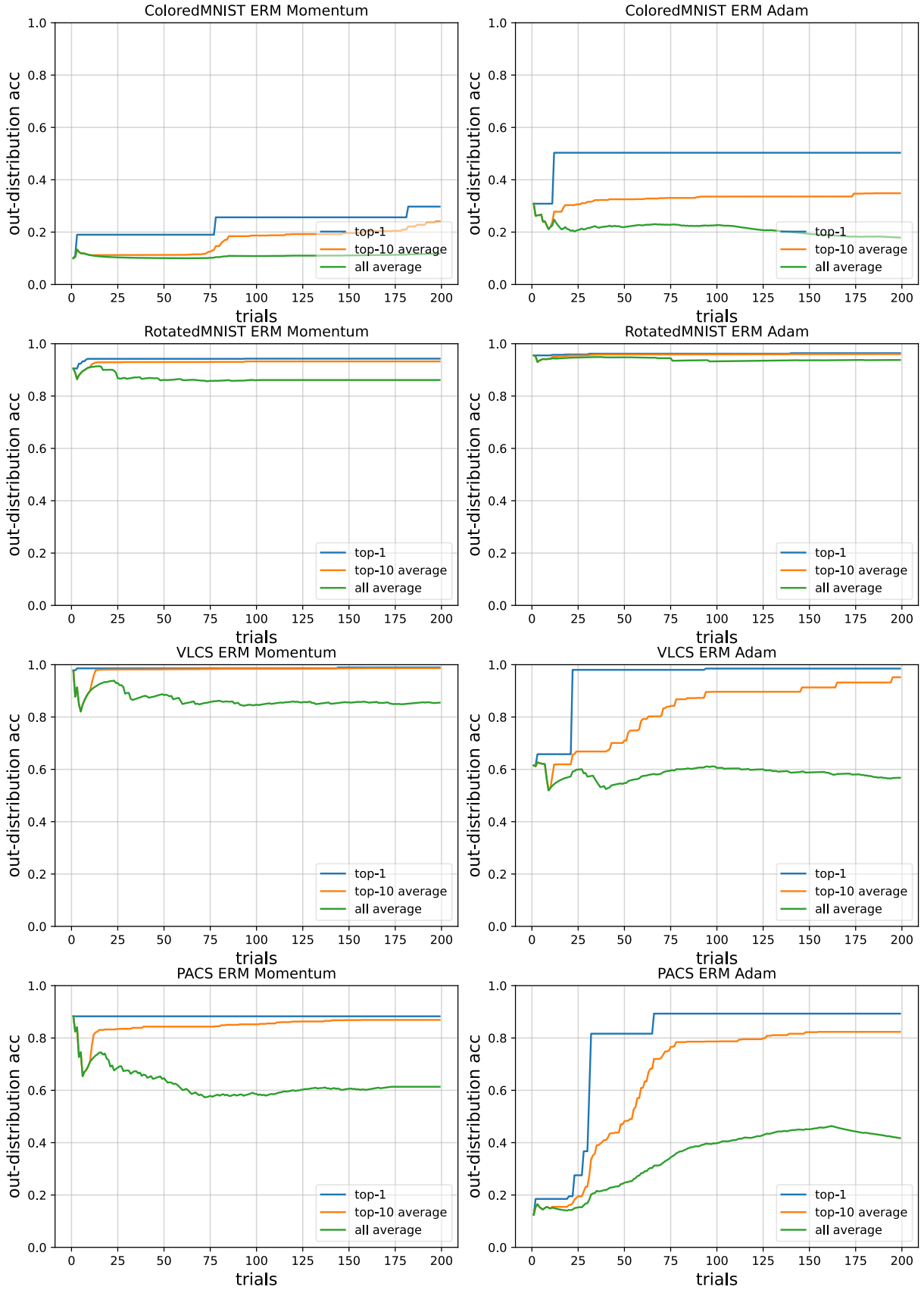

Figure 26. ERM ColoredMNIST, RotatedMNIST, VLCS and PACS / OOD accuracy when horizontal axis is the trial budget

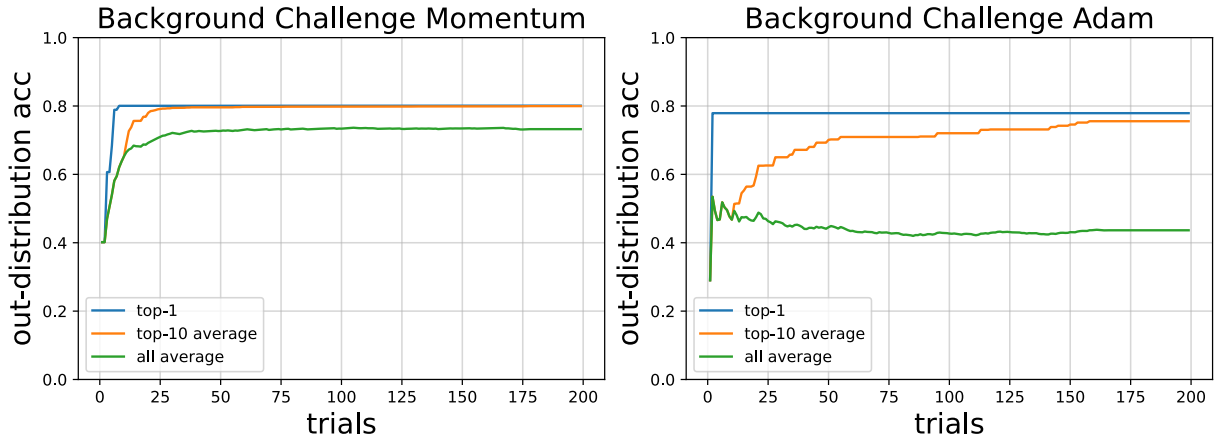

Figure 27. ERM Background Challenge / OOD accuracy when horizontal axis is the trial budget

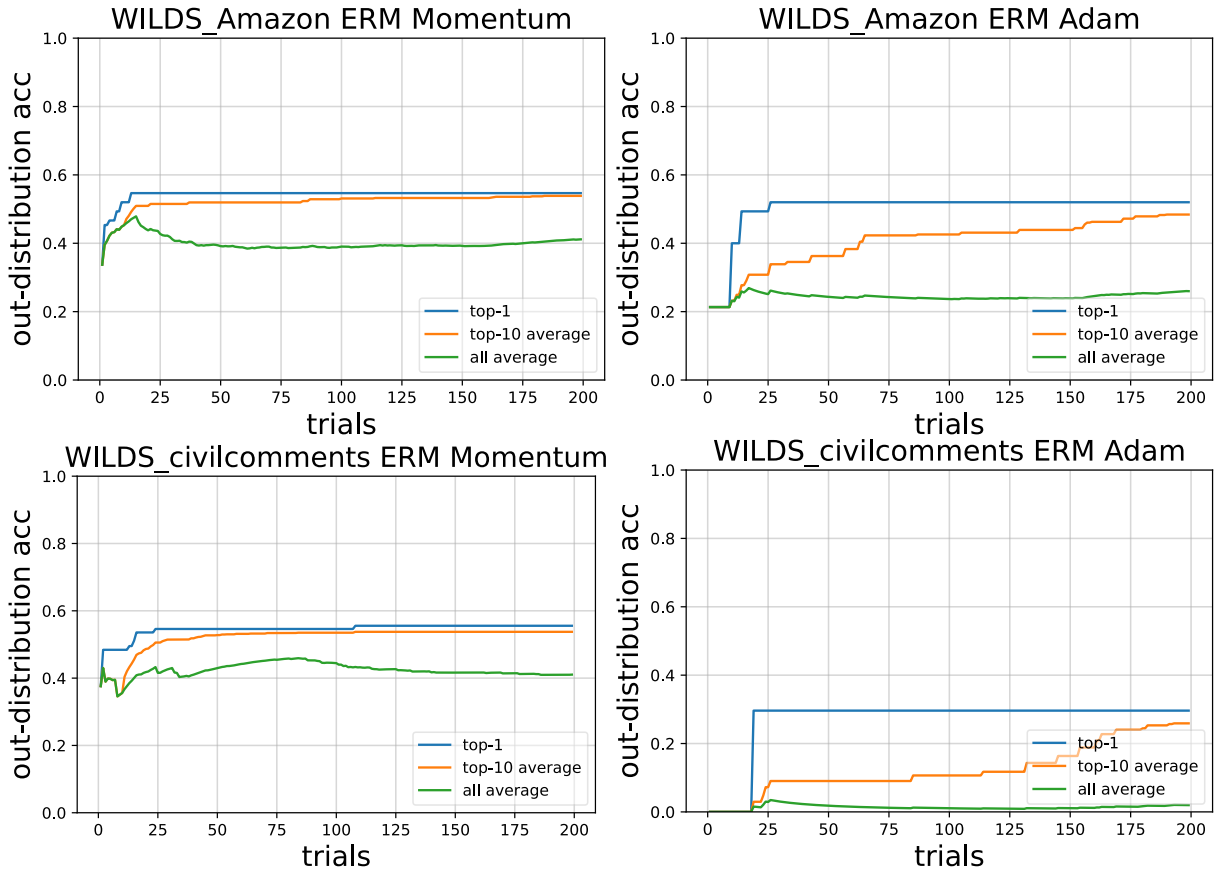

Figure 28. ERM WILDS Amazon and WILDS CivilComment / OOD accuracy when horizontal axis is the trial budget

G.2.2 Hyperparameter Trial Budget vs OOD Error

To visualize the slight increase at the end of OOD accuracy more clearly, we visualized it in log scale as OOD error.

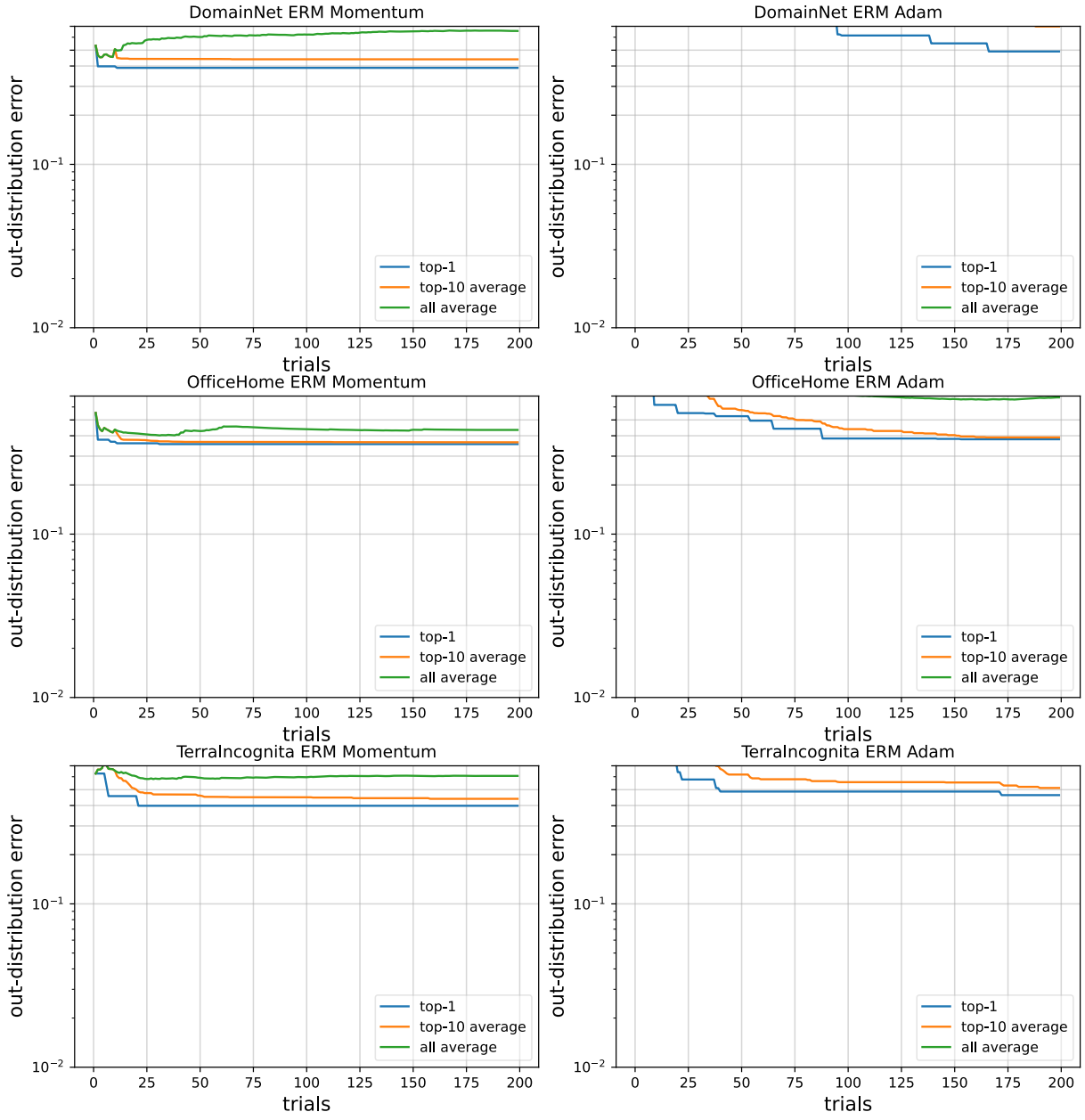

Figure 29. ERM DomainNet, OfficeHome and TerraIncognita / OOD error when horizontal axis is the trial budget

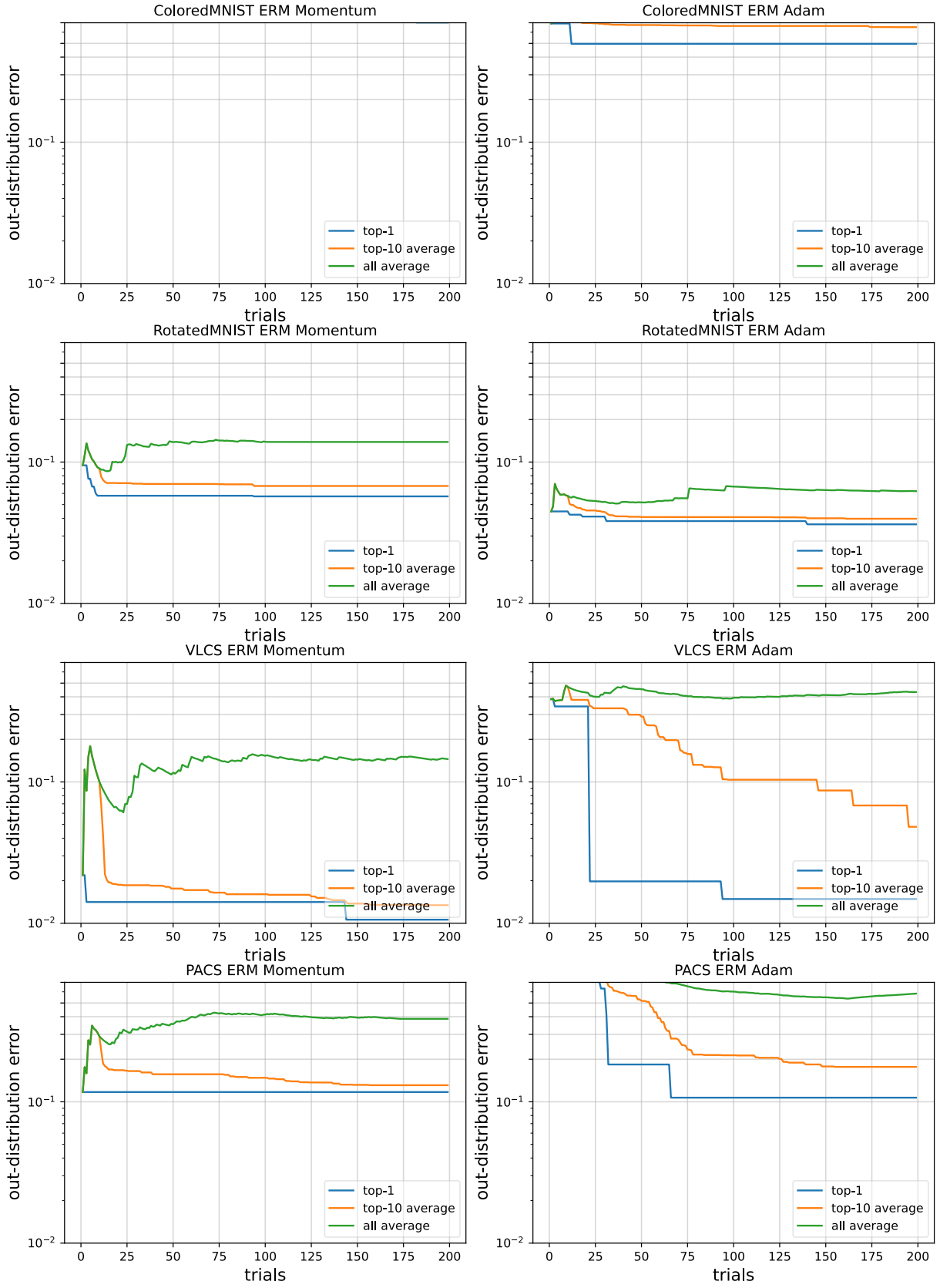

Figure 30. ERM ColoredMNIST, RotatedMNIST, VLCS and PACS / OOD error when horizontal axis is the trial budget

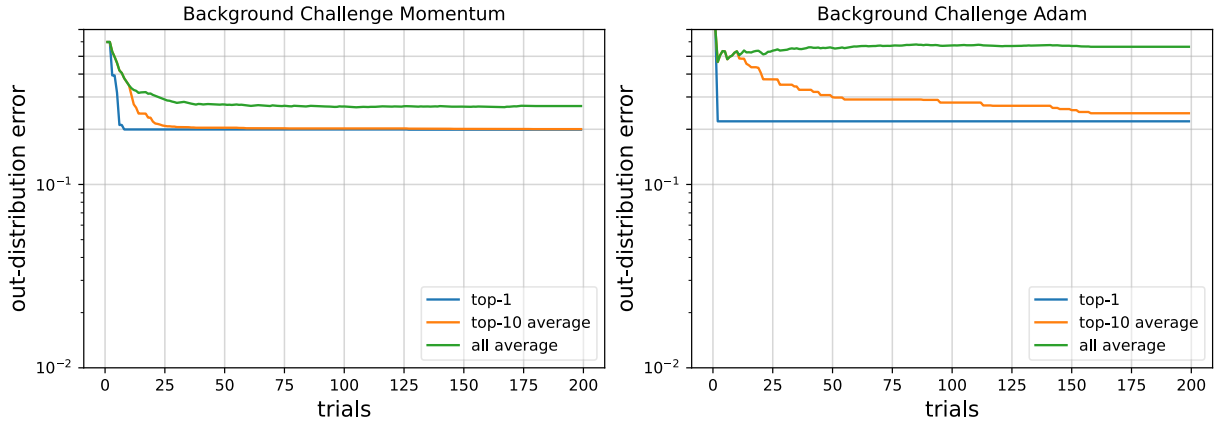

Figure 31. ERM Background Challenge / OOD accuracy when horizontal axis is the trial budget

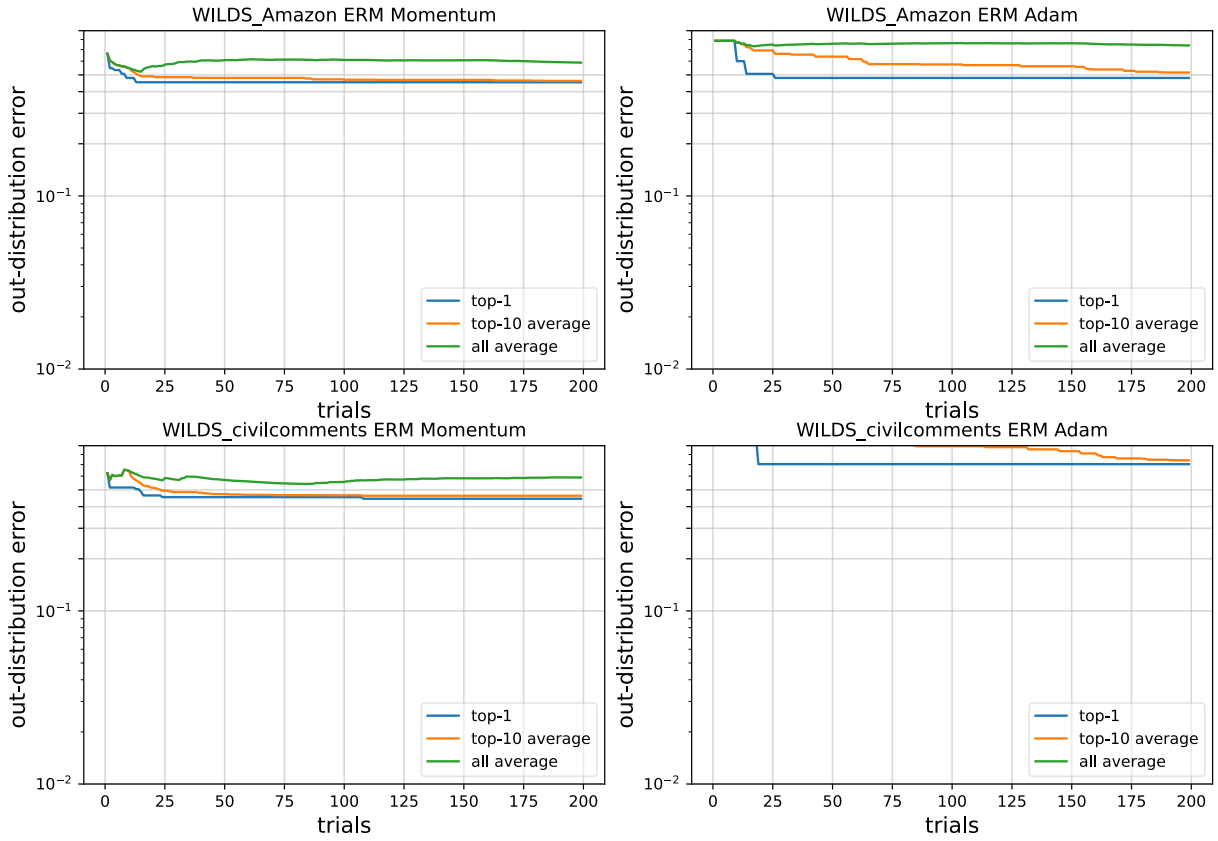

Figure 32. ERM WILDS Amazon and WILDS CivilComment / OOD accuracy when horizontal axis is the trial budget

G.3 Learning Curve of ColoredMNIST

In Section 4.2, we conjecture that the better performance of Adam in Colored MNIST classification may come from overfitting to training data. To confirm this hypothesis, we plot the averaged training accuracy, the averaged validation accuracy, and the averaged test accuracy throughout the training. We pick the top-14 results in terms of test accuracy and use them for the plot. We show the result in Figure 33.

As is evident from Figure 33 (a) and Figure 33 (b), we observe that training accuracy increases while the validation accuracy keeps unchanged. This indicates that overfitting occurs in the training. However, Figure 33 (c) indicates that test accuracy gradually improves as the model is overfitting. On the other hand, SGD shows no such overfitting and OOD generalization improvement, as shown in Figure 34. Thus, we can empirically support our conjecture that Adam produces the better OOD generalization performance by overfitting training data.

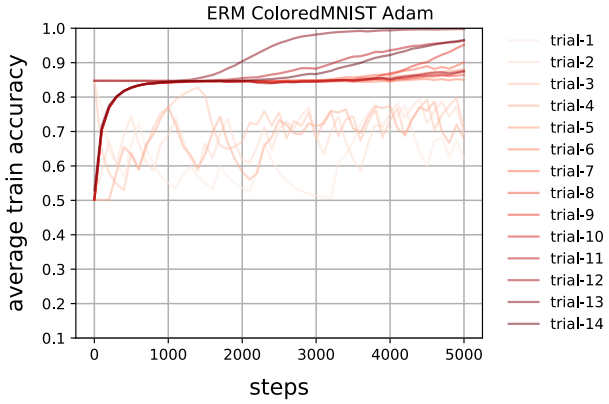

(a) ERM: Averaged training accuracy of Adam on Colored MNIST throughout the training.

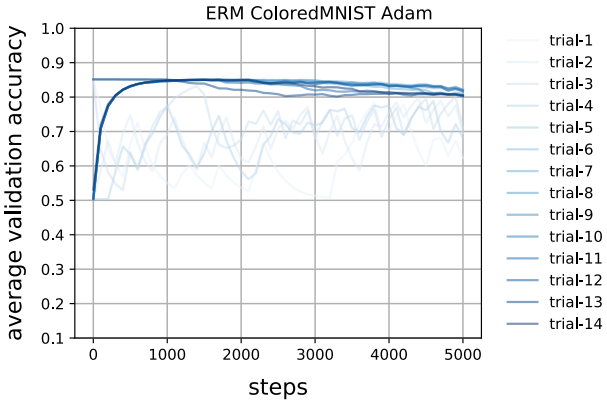

(b) ERM: Averaged validation accuracy of Adam on Colored MNIST throughout the training.

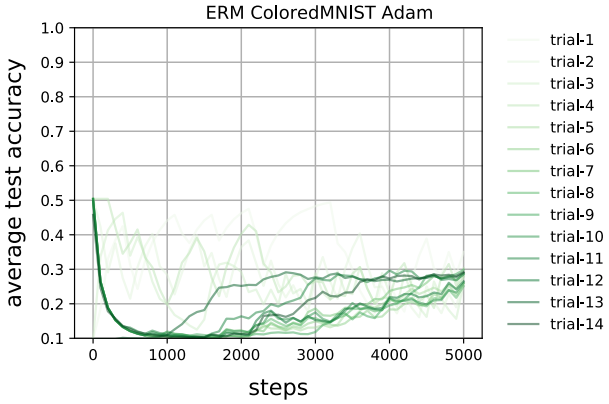

(c) ERM: Averaged test accuracy of Adam on Colored MNIST throughout the training.

Figure 33. Adam: Comparison of averaged training accuracy, averaged validation accuracy, and averaged test accuracy throughout the training. We plot these values of check points whose train accuracy is in the top-14.

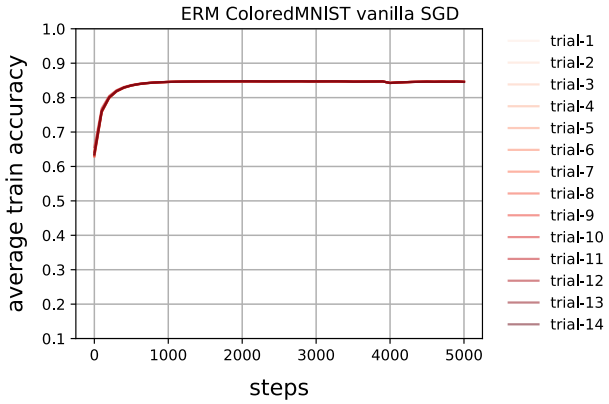

(a) ERM: Averaged training accuracy of SGD on Colored MNIST throughout the training.

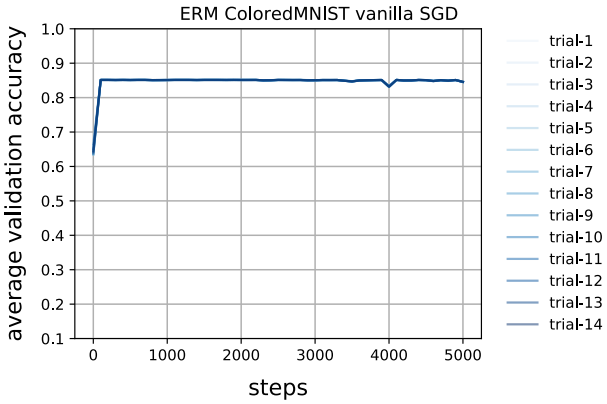

(b) ERM: Averaged validation accuracy of SGD on Colored MNIST throughout the training.

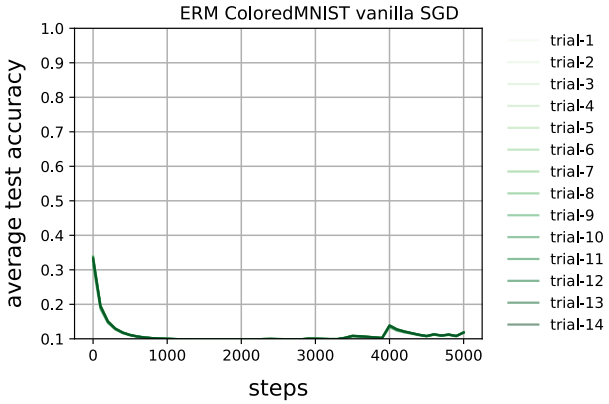

(c) ERM: Averaged test accuracy of SGD on Colored MNIST throughout the training.

Figure 34. SGD: Comparison of averaged training accuracy, averaged validation accuracy, and averaged test accuracy of SGD throughout the training. We plot these values of checkpoints whose train accuracy is in the top-14.

G.4 Early Stopping

In Section 4.2, figures 1 shows that adaptive optimizers tend to overfit to training domain. A possible reason is that the training speed of adaptive methods is faster than non-adaptive ones. That is, in the same steps budget, adaptive optimizers converge faster in effect. To validate if this is the case, we investigate whether early stopping improves the OOD generalization of adaptive optimizers.

In particular, we compute the difference between averaged accuracy at early stopping and at last epoch for test accuracy and validation accuracy, respectively:

$$Acc_{\text{diff}} = \frac{1}{N_{\text{es}}} \sum_{i=1}^{N_{\text{es}}} Acc_{\text{es-i}} - \frac{1}{N_{le}} \sum_{i=1}^{N_{\text{le}}} Acc_{\text{le-i}} \tag{18}$$

where Acc_{diff} represents the difference in accuracy between early stopping and the last epoch, N_{es} is the number of trials at early stopping, N_{le} is the number of trials at the last epoch, $Acc_{\text{es-i}}$ denotes the accuracy at the early stopping for the $i-th$ trial, $Acc_{\text{le-i}}$ denotes the accuracy at the last epoch for the $i-th$ trial.

If the average accuracy at early stopping is larger, the difference is positive and vice versa.

Figures 35 to 40 are the results of this comparison for each dataset and algorithm. The y-axis is the difference of out-of-distribution (test) accuracy and the x-axis is the difference of in-distribution (validation) accuracy. The color indicates the epoch of early stopping. The darker color indicates that early stopping is conducted in relatively earlier epochs.

For PACS, both differences are positive and lighter colors are concentrated at points of small difference of the validation accuracy, as indicated in Figures 35 and 36. Therefore, we can conclude that when the validation accuracy deteriorates by further training, the test accuracy also gets worse. However, the effect of further training is less evident for Adam. In other words, early stopping does not influence Adam so much but keeps test accuracy from decreasing for SGD.

The result of VLCS shows a similar pattern as PACS (Figures 37 and 38). If anything, Further training after early stopping makes adaptive optimizes be likely to result in better test accuracy than SGD, though they have a large variance. With respect to SGD, additional training degrades the test accuracy as much as it degrades validation accuracy.

Office-Home shows similar results as PACS, as presented in Figures 39 and 40.

In summary, we find that early stopping does not influence adaptive optimizers. Therefore, we can conclude that adaptive optimizer overfits not because it trains faster than non-adaptive methods.

The fact that early stopping does not affect the adaptive optimizer means that adjusting the number of epochs instead of a fixed number of epochs will not change the result. We have followed previous studies and experimented with a fixed number of epochs in the present study, and our results suggest that this does not have a serious impact on the comparison of adaptive and non-adaptive optimizers. Thus, we can see that using a fixed epoch number does not undermine the validity of our optimizer comparison experiment in this sense.

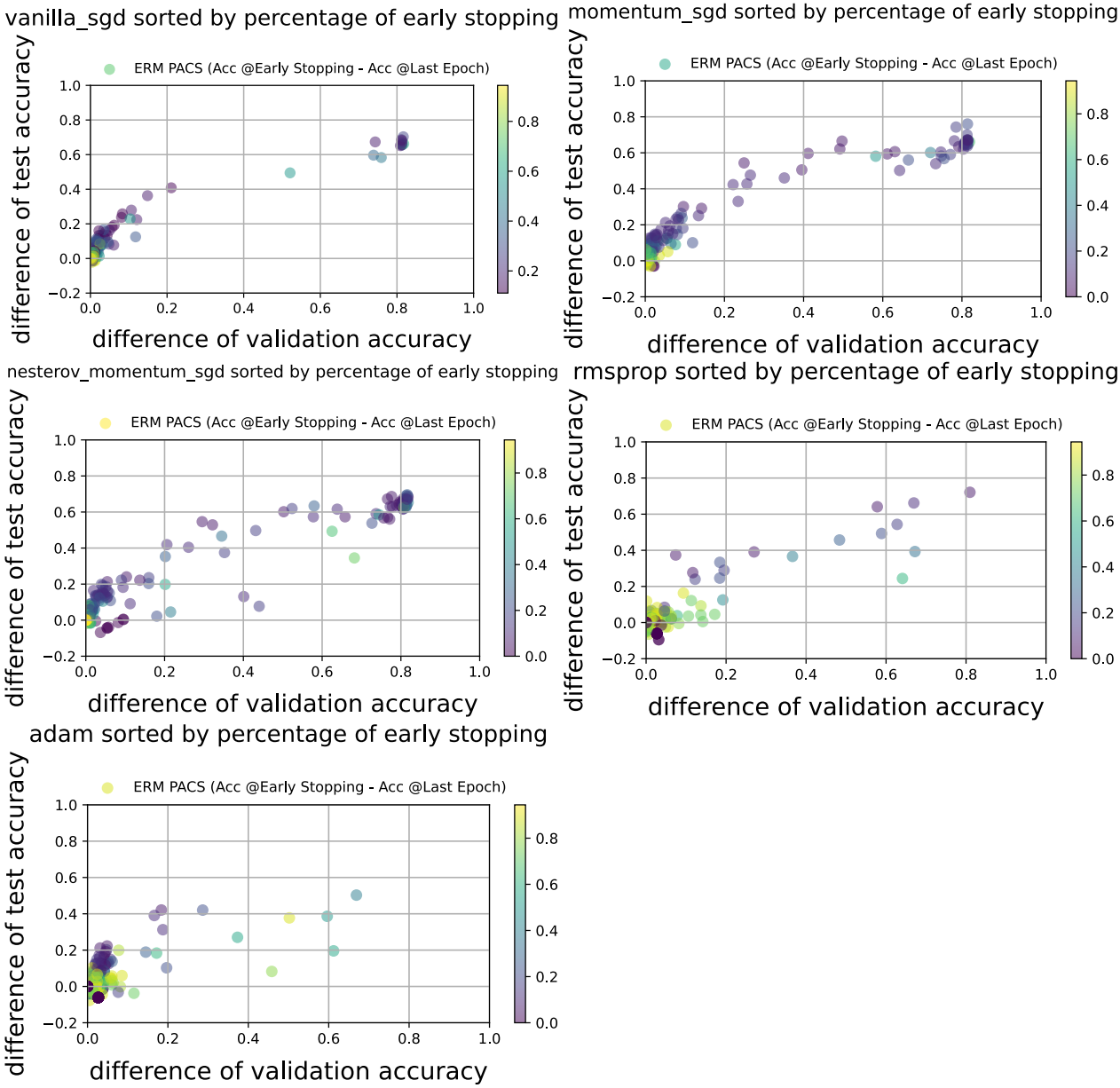

Figure 35. ERM/PACS: Difference between accuracy at early stopping and at last epoch. The y-axis is the difference of out-of-distribution (test) accuracy and the x-axis is the difference of in-distribution (validation) accuracy. The color indicates the epoch of early stopping. The darker color indicates that early stopping is conducted in relatively earlier epochs.

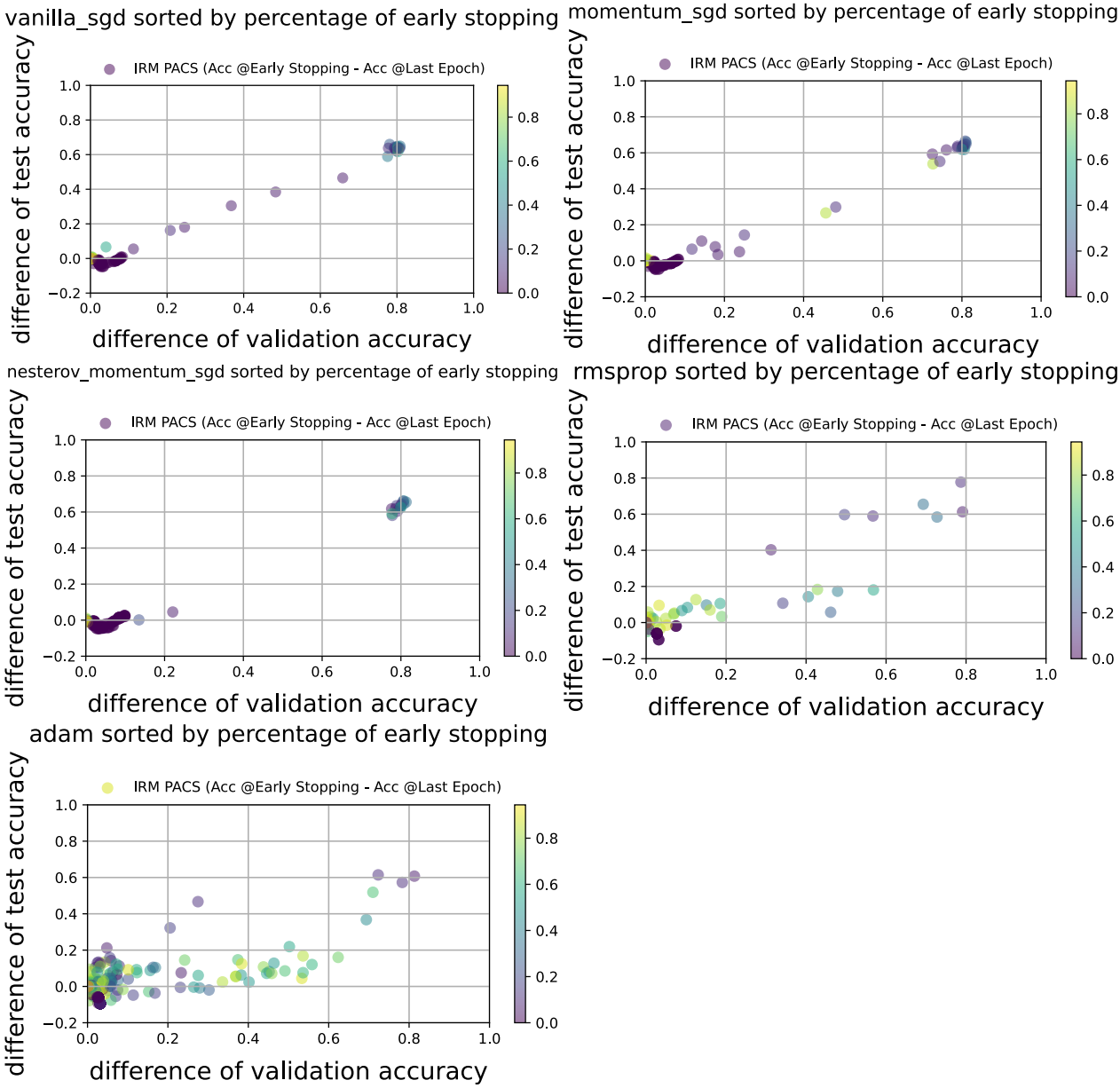

Figure 36. IRM/PACS: Difference between accuracy at early stopping and at last epoch. The y-axis is the difference of out-of-distribution (test) accuracy and the x-axis is the difference of in-distribution (validation) accuracy. The color indicates the epoch of early stopping. The darker color indicates that early stopping is conducted in relatively earlier epochs.

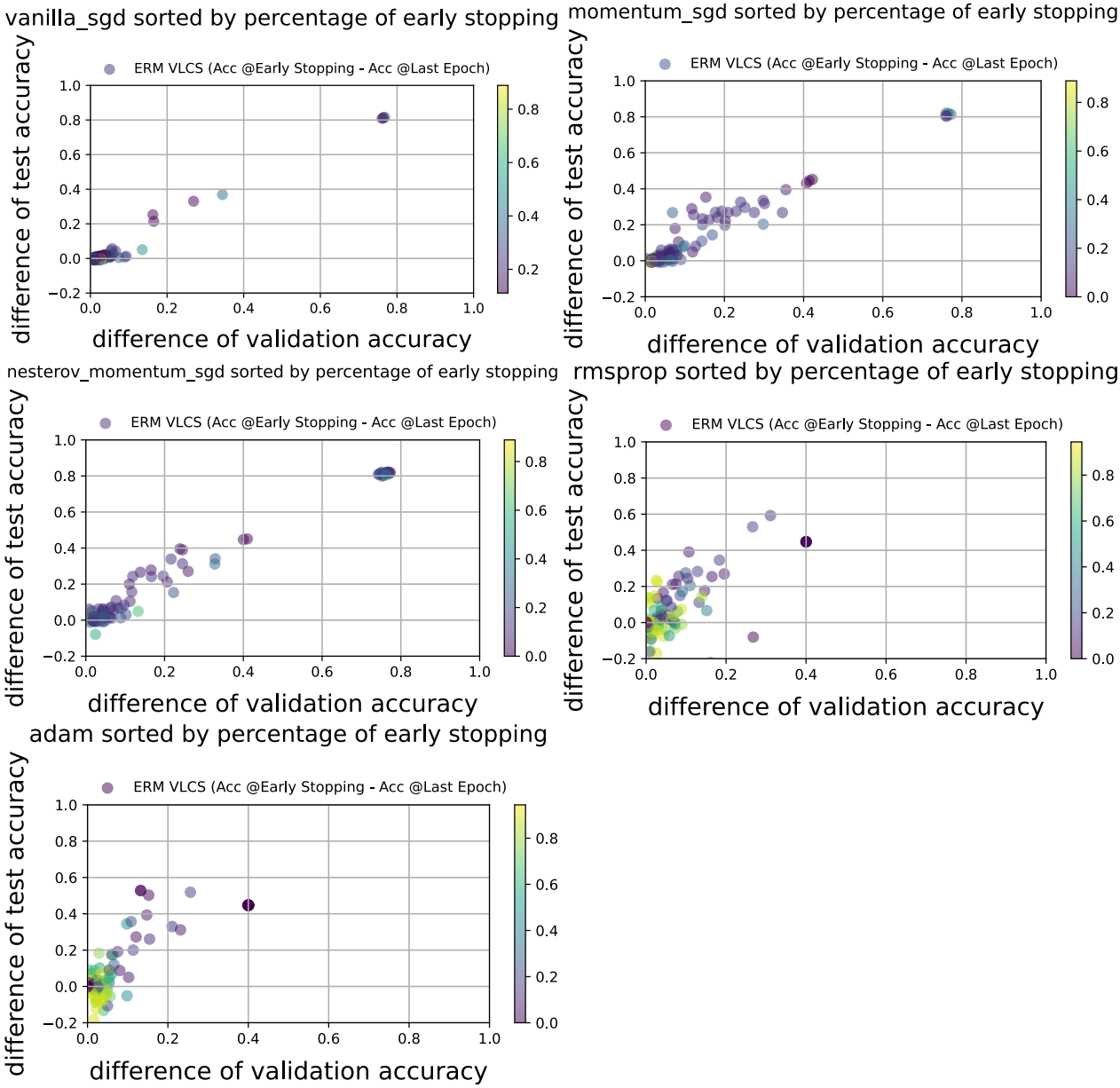

Figure 37. ERM/VLCS: Difference between accuracy at early stopping and at last epoch. The y-axis is the difference of out-of-distribution (test) accuracy and the x-axis is the difference of in-distribution (validation) accuracy. The color indicates the epoch of early stopping. The darker color indicates that early stopping is conducted in relatively earlier epochs.

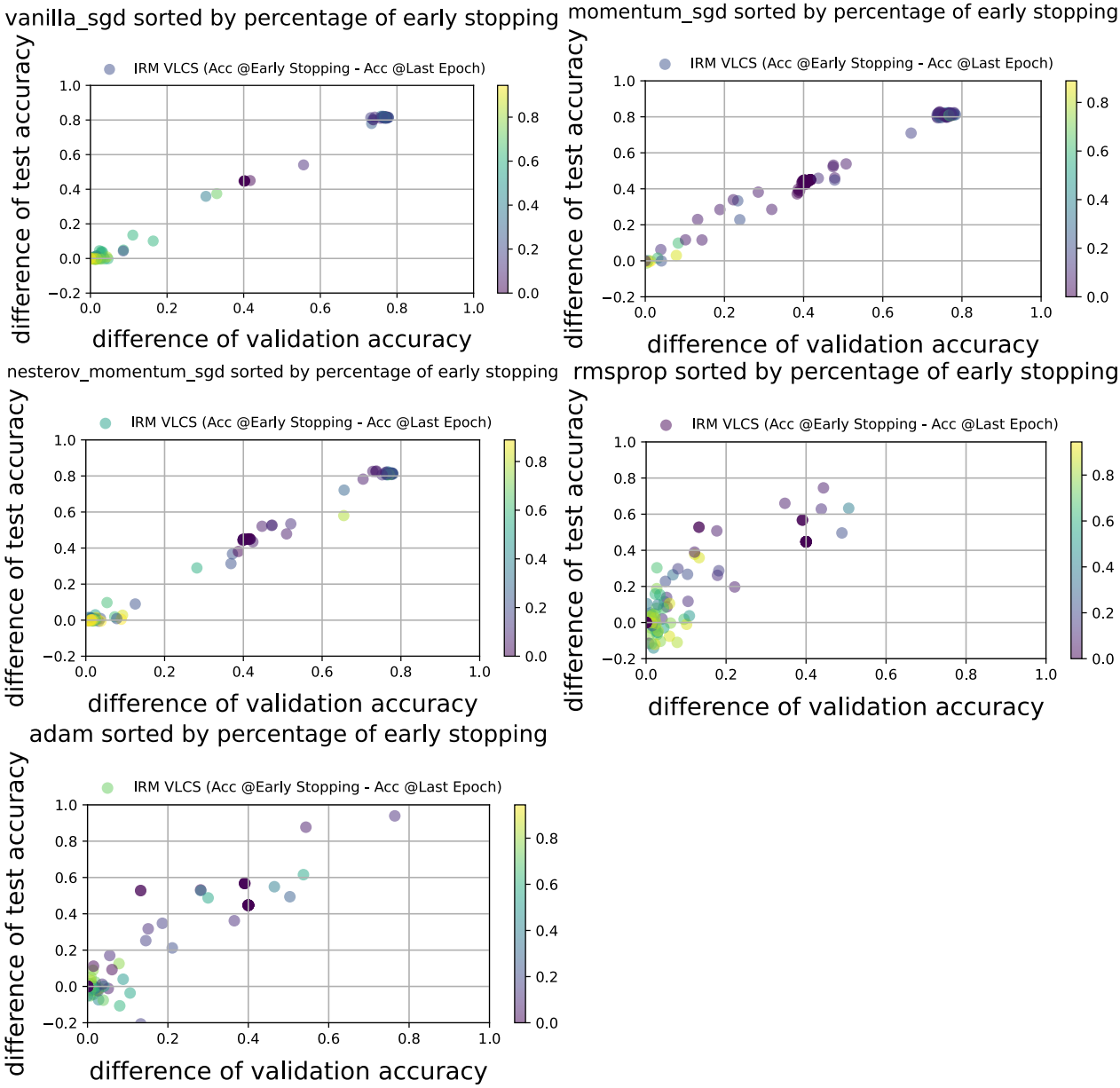

Figure 38. IRM/VLCS: Difference between accuracy at early stopping and at last epoch. The y-axis is the difference of out-of-distribution (test) accuracy and the x-axis is the difference of in-distribution (validation) accuracy. The color indicates the epoch of early stopping. The darker color indicates that early stopping is conducted in relatively earlier epochs.

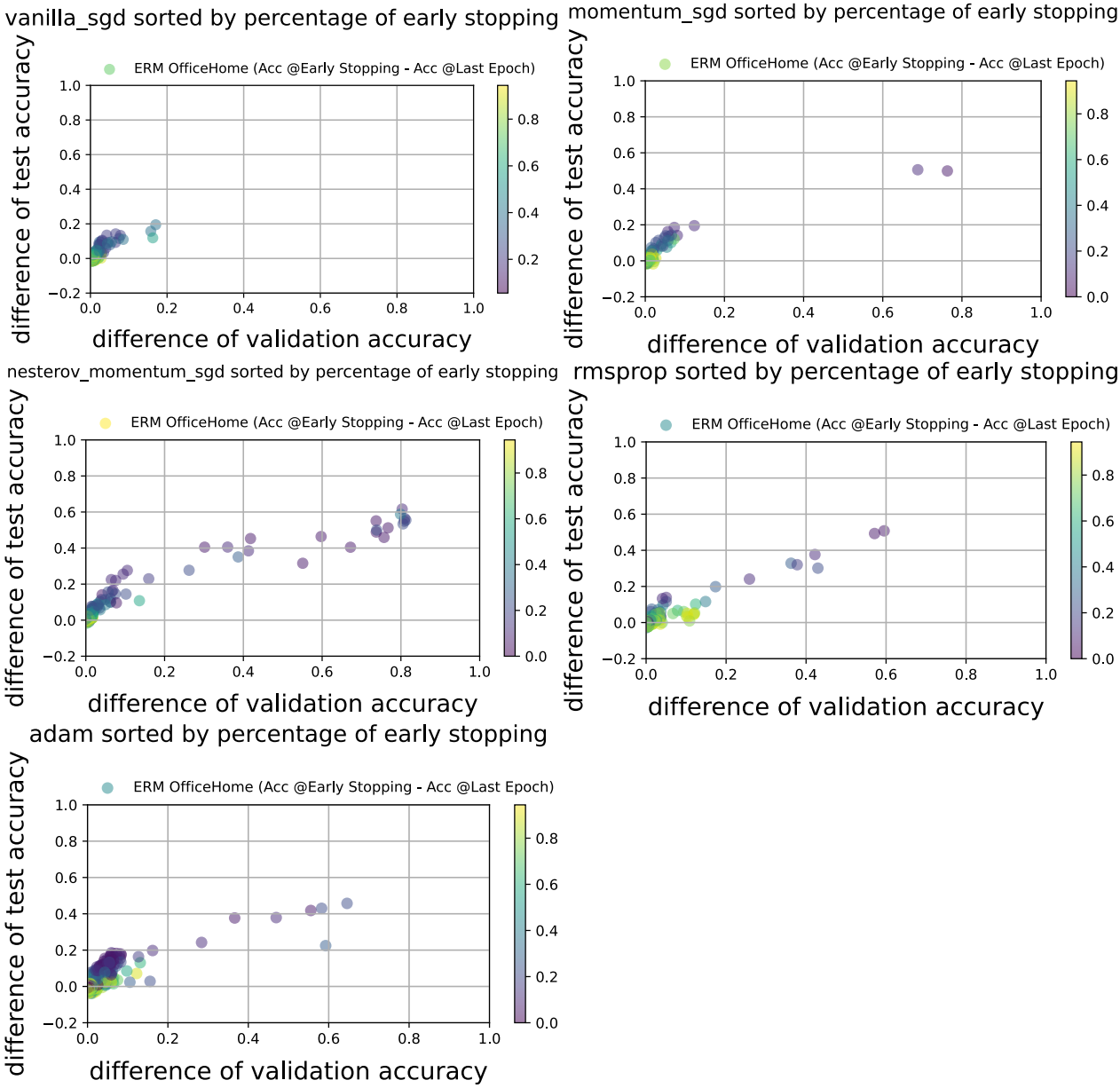

Figure 39. ERM/Office-Home: Difference between accuracy at early stopping and at last epoch. The y-axis is the difference of out-of-distribution (test) accuracy and the x-axis is the difference of in-distribution (validation) accuracy. The color indicates the epoch of early stopping. The darker color indicates that early stopping is conducted in relatively earlier epochs.

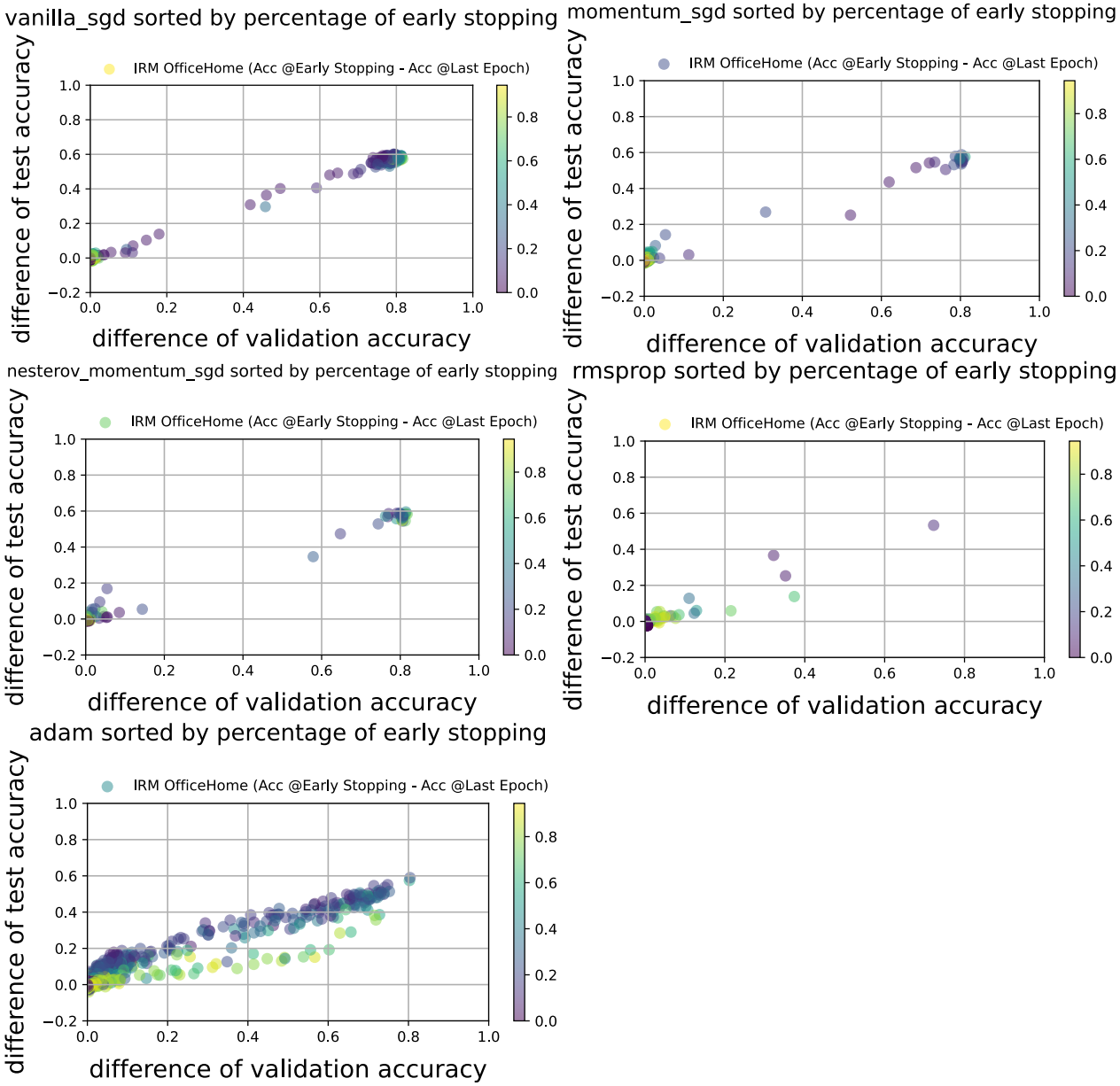

Figure 40. IRM/Office-Home: Difference between accuracy at early stopping and at last epoch. The y-axis is the difference of out-of-distribution (test) accuracy and the x-axis is the difference of in-distribution (validation) accuracy. The color indicates the epoch of early stopping. The darker color indicates that early stopping is conducted in relatively earlier epochs.

However, we find different results from Colored MNIST. As shown in Figures 41 and 42, we can observe that the difference of validation accuracy is positive and that of test accuracy is negative. That is further training after early stopping decreases validation accuracy but increases test accuracy on Colored MNIST, while there is no difference for SGD. This is consistent with the result of Appendix G.3.

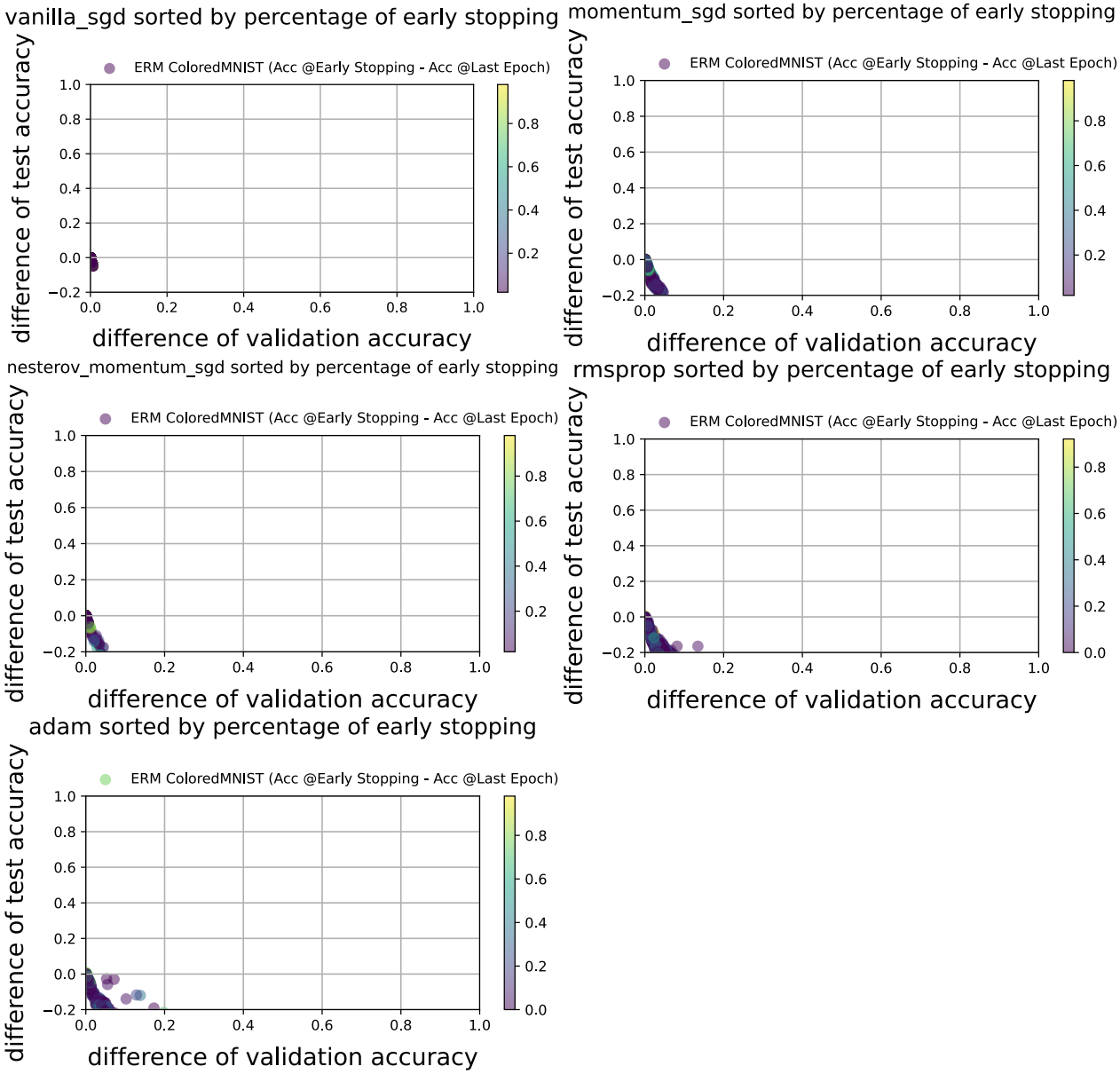

Figure 41. ERM/Colored MNIST: Difference between accuracy at early stopping and at last epoch. The y-axis is the difference of out-of-distribution (test) accuracy and the x-axis is the difference of in-distribution (validation) accuracy. The color indicates the epoch of early stopping. The darker color indicates that early stopping is conducted in relatively earlier epochs.

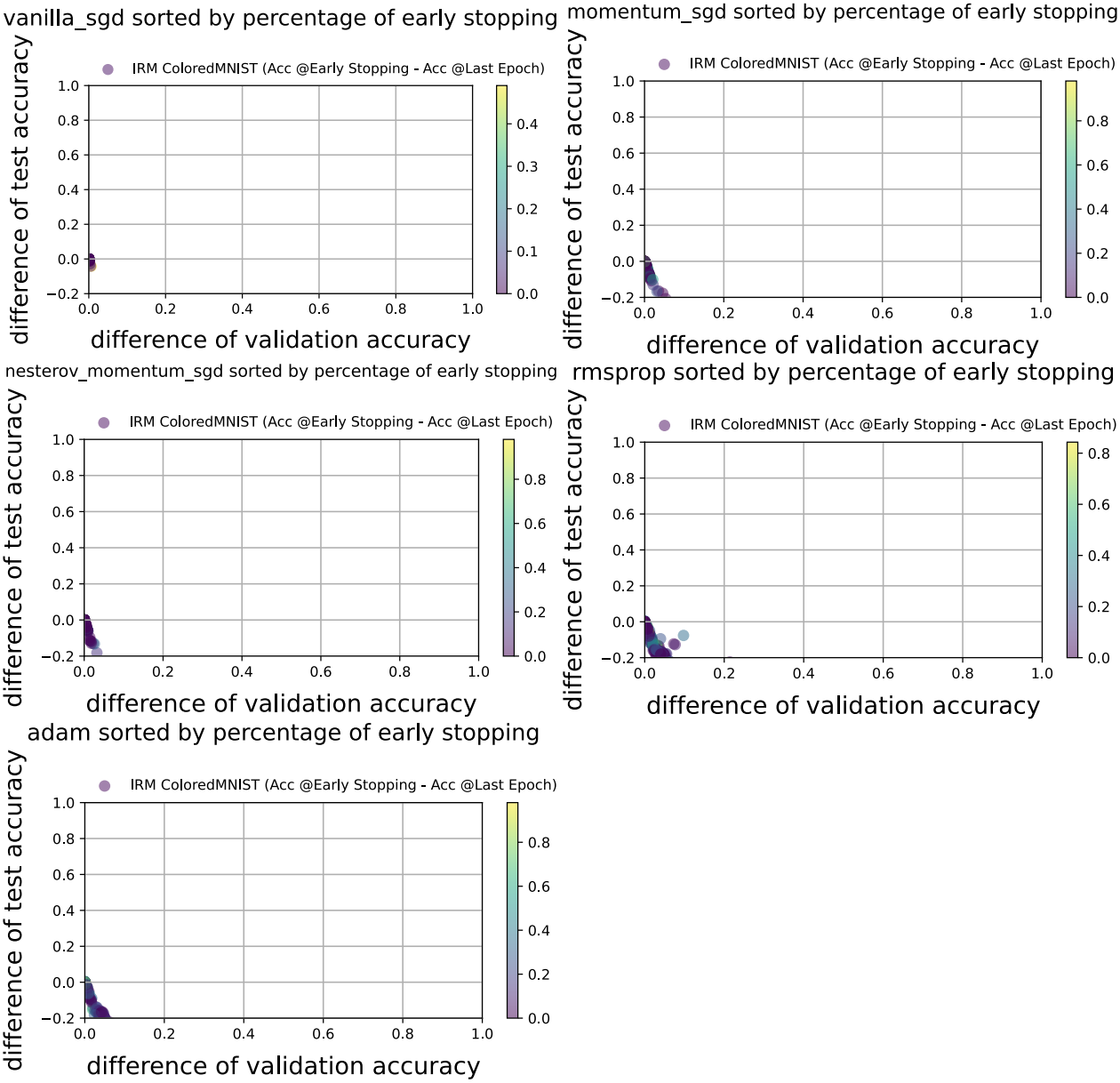

Figure 42. IRM/Colored MNIST: Difference between accuracy at early stopping and at last epoch. The y-axis is the difference of out-of-distribution (test) accuracy and x-axis is the difference of in-distribution (validation) accuracy. The color indicates the epoch of early stopping. The darker color indicates that early stopping is conducted in relatively earlier epochs.

H Soundness Check of Our Experiments

H.1 Histgram of Hyperparameters

We have shown the histgram of the hyperparameters to be used for training just for reference. In particular, we display a result for learning rate of Momentum SGD and Adam for the each dataset. We observe that we could sample hyperparameters from a reasonably wide range.

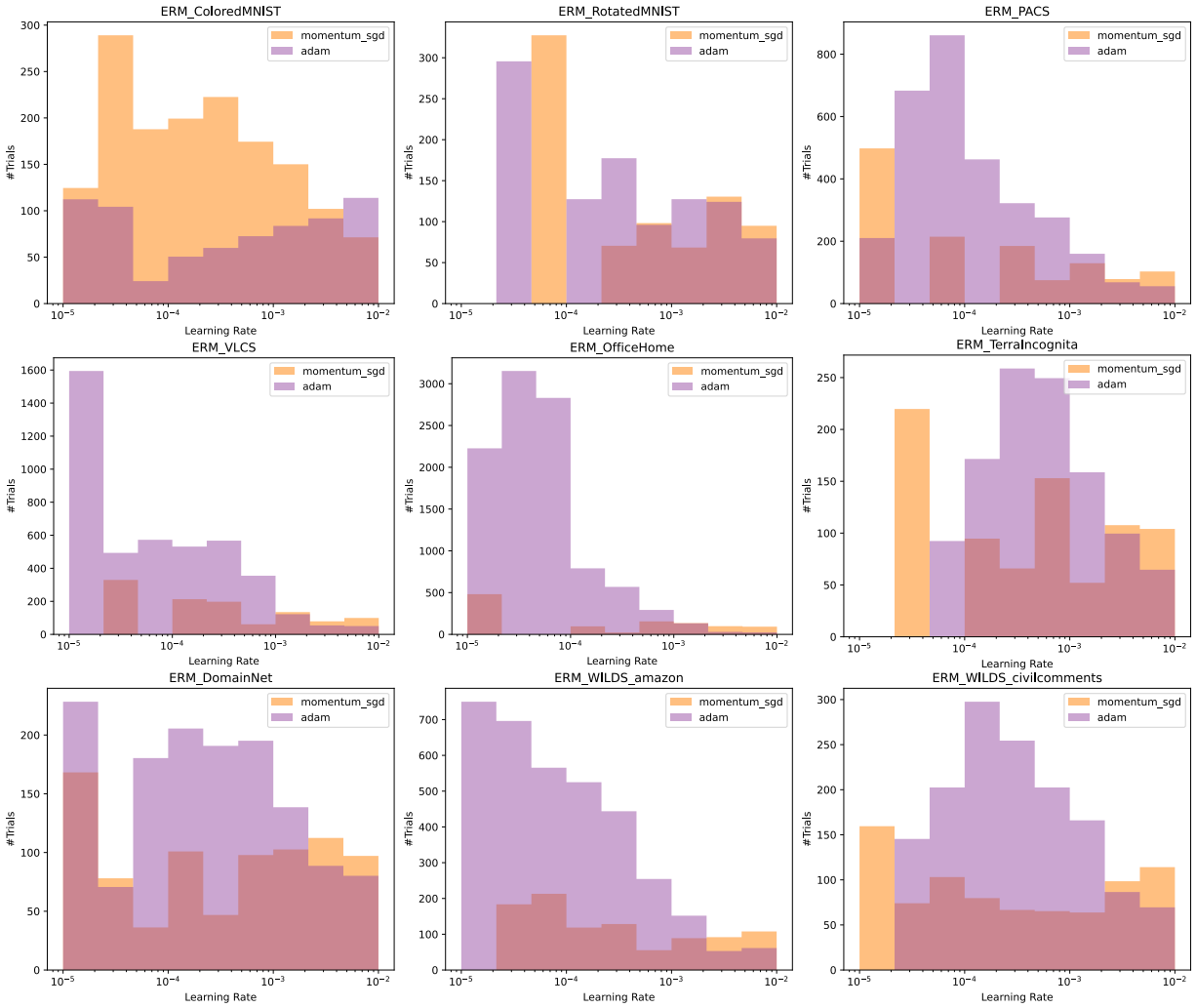

Figure 43. Histogram of explored hyperparameters (learning rate) in training of DomainBed, WILDS dataset in ERM. Momentum SGD and Adam results are included. Although uniform distribution is used as the prior distribution for hyperparameter optimization, the histogram results do not match the uniform distribution because Bayesian optimization is used.

H.2 Hyperparameters and OOD Accuracy Box-Plot

The previous section provided information on the hyperparameter search range. In this section, we share the results of the out-of-distribution performance for a specific hyperparameter range as a box plot with the hyperparameters separating the bin as shown in Figure 44, 45 and 46.

From these results, we observe that lr, which achieves high out-of-distribution accuracy, is within the search range of learning rate and thus has sufficient range to perform the search.

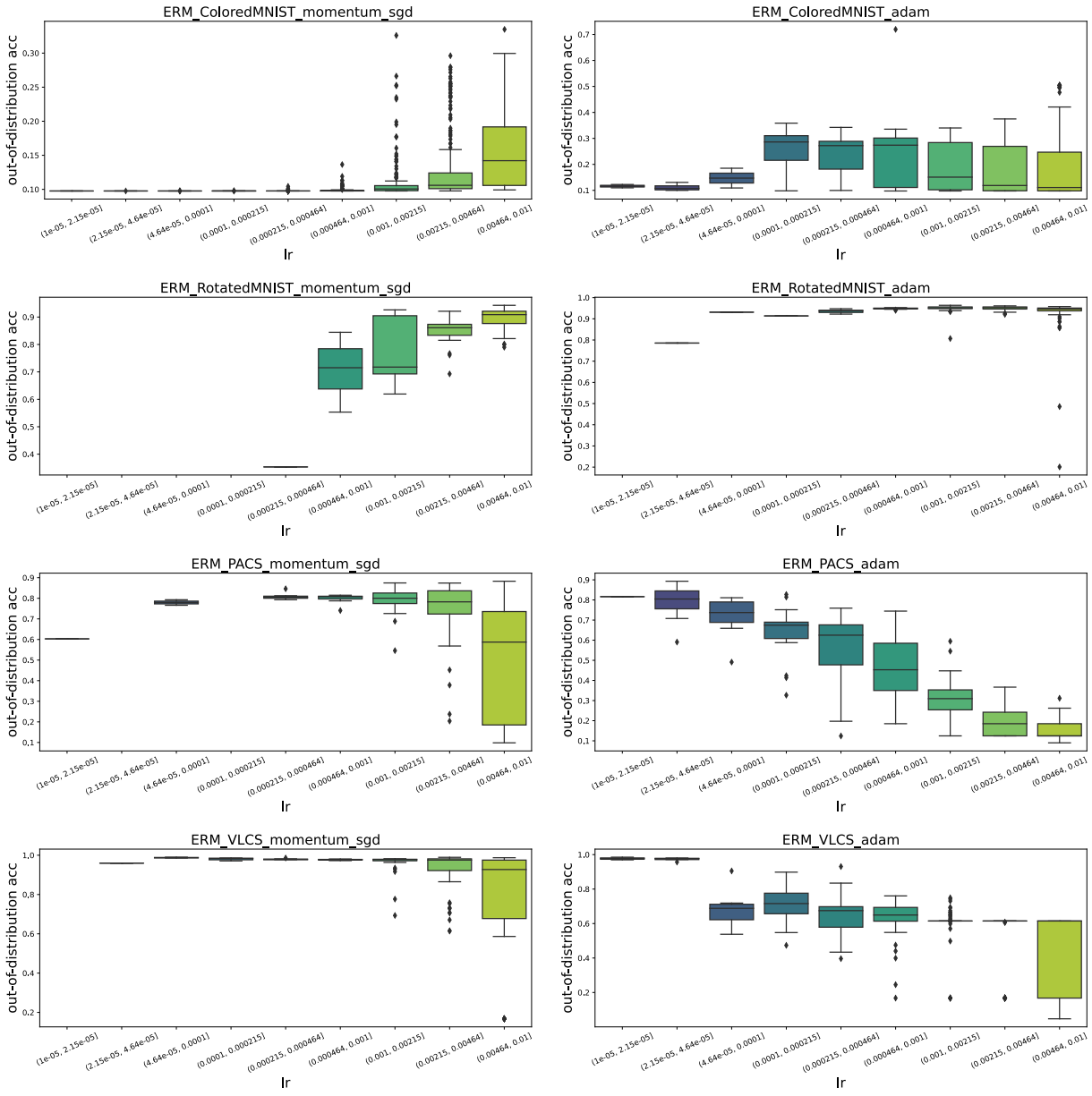

Figure 44. Box-Plot of Out-of-Distribution Accuracy per Log-Scale of Learning Rate: ColoredMNIST, RotatedMNIST, PACS and VLCS

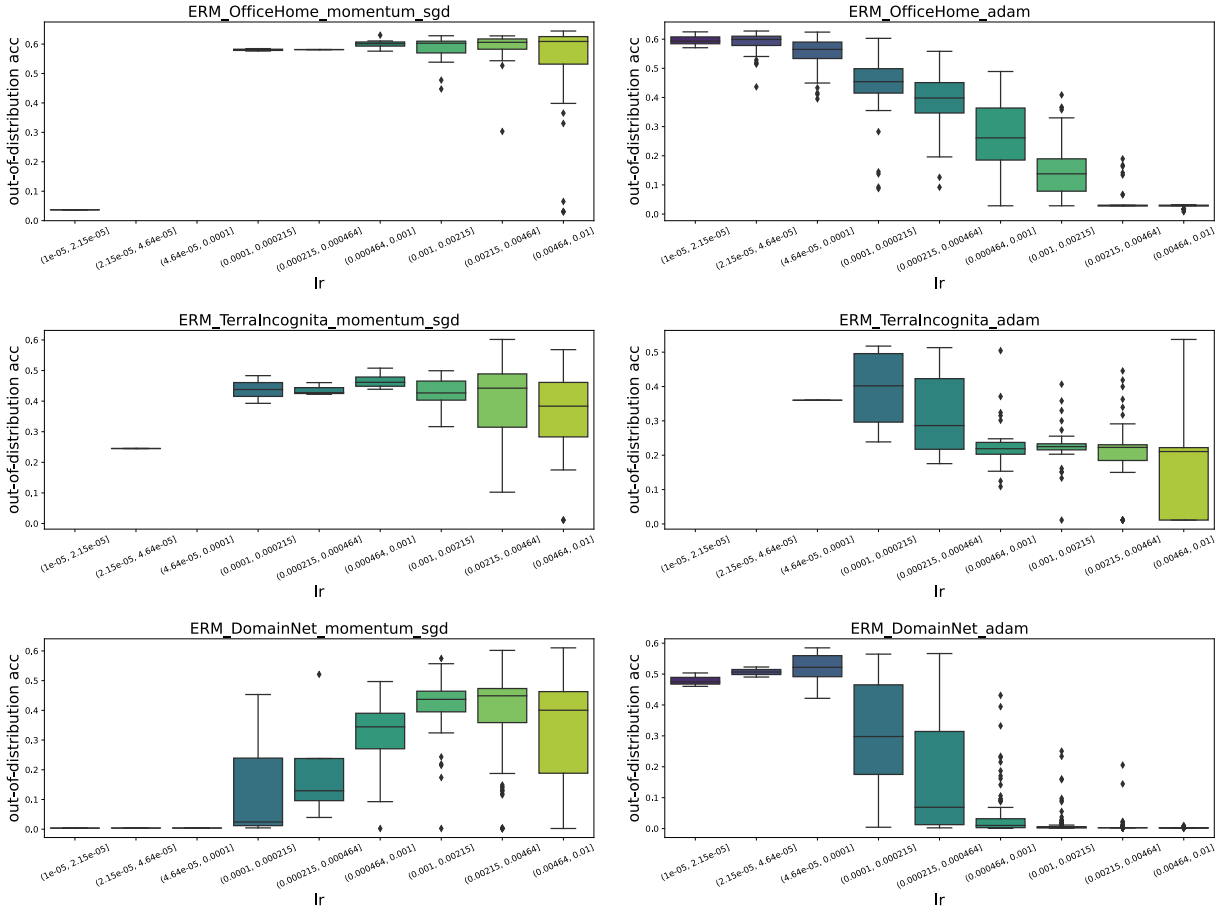

Figure 45. Box-Plot of Out-of-Distribution Accuracy per Log-Scale of Learning Rate: OfficeHome, TerraIncognita, and DomainNet

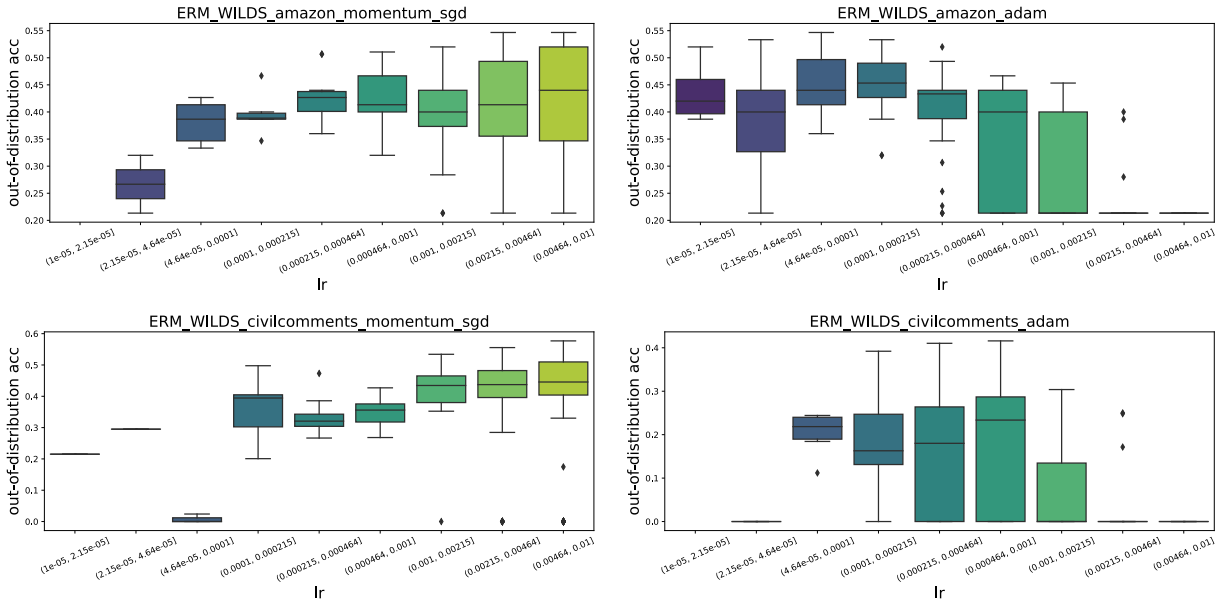

Figure 46. Box-Plot of Out-of-Distribution Accuracy per Log-Scale of Learning Rate: Amazon-WILDS, and CivilComments-WILDS

H.3 Effect of Initial Configuration on Hyperparameter Optimization

In this section, we investigate how the first hyperparameter combination affected the search in our Bayesian optimization of hyperparameters. We compared Momentum SGD to Adam and chose PACS as our dataset. The experimental results showed that random initialization which we used, given a sufficient number of trials (e.g., more than 200 trials within our experimental protocol), did not differ from the final performance obtained when searching from the default hyperparameters of pytorch.

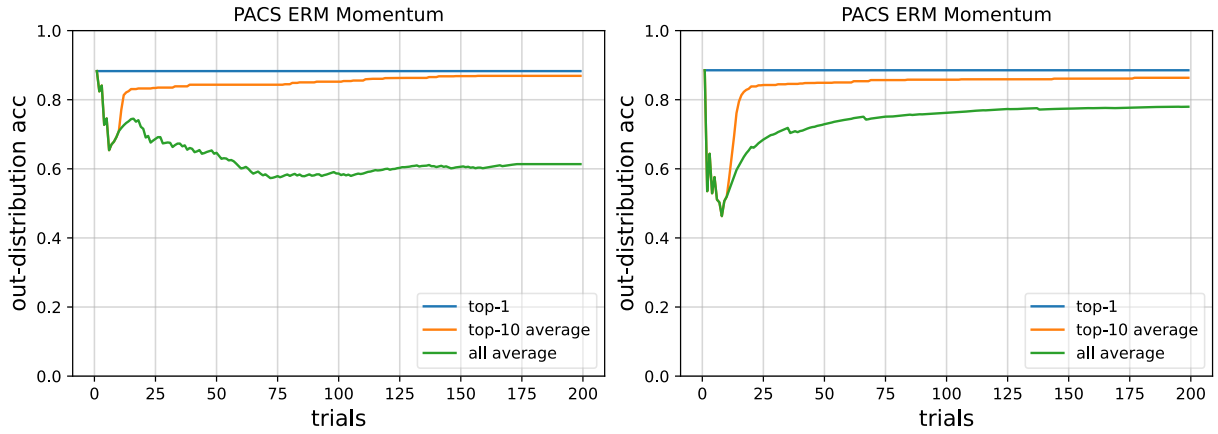

Figure 47. ERM PACS MomentumSGD / Comparison of Initialization (Left: Random initialization, Right: Pytorch default hyperparameter initialization)

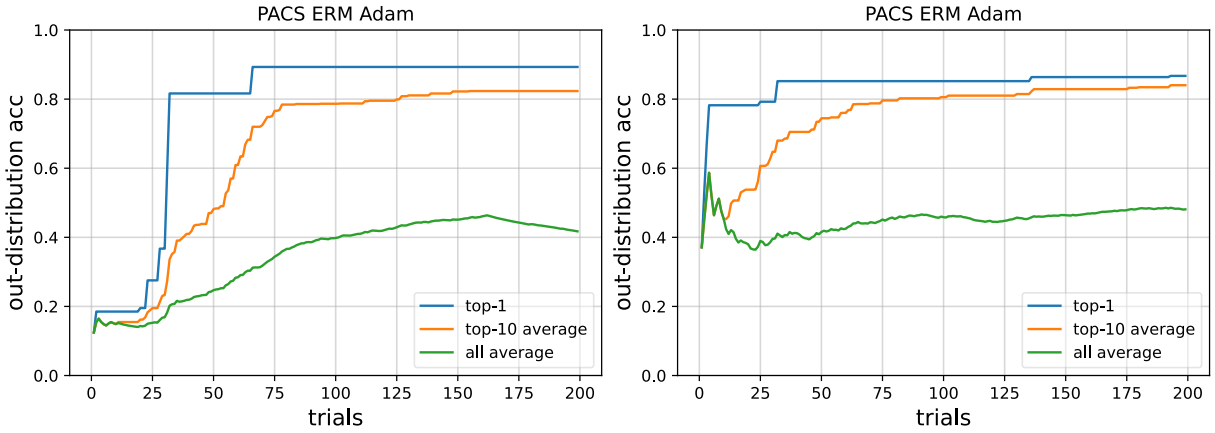

Figure 48. ERM PACS Adam / Comparison of Initialization (Left: Random initialization, Right: Pytorch default hyperparameter initialization)

H.4 Best OOD Performance Comparison against with Existing Benckmark

In order to confirm the soundness of our experiments, we compared our results with existing benchmarks to see how well they actually performed, in addition to the hyperparameter search ranges in the previous section. In particular, we compared our experimental results with those of DomainBed (Gulrajani & Lopez-Paz, 2021), an existing oracle benchmark that uses Adam.

Table 15: OOD accuracy (%) comparison of our experimental results with the benchmark results reported in DomainBed (Gulrajani & Lopez-Paz, 2021)

Dataset	OOD Domain	Existing Benchmark Results(Adam)	Our Results(Adam)
ColoredMNIST	0.9	$30.0_{\pm 0.3}$	73.92
RotatedMNIST	0	$96.0_{\pm 0.2}$	96.40
VLCS	C	$97.7_{\pm 0.3}$	99.36
PACS	A	$87.8_{\pm 0.4}$	89.30
OfficeHome	A	$61.2_{\pm 1.4}$	63.12
TerraIncognita	L100	$59.9_{\pm 1.0}$	61.35
DomainNet	clipart	$58.4_{\pm 0.3}$	58.48

I Additional Study

I.1 Corruption and Perturbation Shift

In the main body of our paper, we presented experimental results for the seven types of domain shifts included in DomainBed (Gulrajani & Lopez-Paz, 2021), as well as the Background Challenge (Xiao et al., 2021), which deals with background shifts, and WILDS datasets (Koh et al., 2021) which deals with the population shift dataset. In this section, we report the results of our investigation of the corruption and perturbation datasets to investigate a broader range of out-of-distribution generalization. Details of the experiments are described in Appendix C.4, D.4 and E.4. CIFAR10-C and CIFAR10-P (Hendrycks & Dietterich, 2019) were used as the datasets. Momentum SGD and Adam were used as optimization methods for comparison.

The CIFAR10-C results are averaged performance results for 19 different noise types of corruption and are based on Hendrycks & Dietterich (2019) experimental protocol. The higher the performance, the better. The CIFAR10-P experiment shows the variability of inference for noise perturbations, with lower values indicating better performance. Experimental results show that Momentum SGD outperforms Adam in both CIFAR10-C and CIFAR10-P (Table 16).

Table 16: CIFAR-10-C (averaging corruption classification accuracy %) and CIFAR-10-P (top-5 robustness perturbation): Performance comparison between Momentum SGD and Adam with mean and standard deviation.

Dataset	Momentum	Adam
CIFAR10-C (↑)	$\mathbf{42.89_{\pm 6.66}}$	$42.06_{\pm 6.79}$
CIFAR10-P (↓)	$\mathbf{1.38_{\pm 0.33}}$	$1.62_{\pm 0.26}$

I.2 Model Architecture

In DomainBed experiments, we followed Gulrajani & Lopez-Paz (2021) and used only ConvNet for the MNIST-based dataset and ResNet-50 for the ImageNet-based dataset. In this section, we investigate the impact of changing the model architecture.

I.2.1 ResNet-20 for ColoredMNIST

Here are the results of ResNet-20 on the ColorMNIST Task (Figure 17). In ConvNet case, Adam outperformed Momentum SGD, but the results were reversed in ResNet-20.

Table 17: ColoredMNIST: OOD accuracy (%) comparison between Momentum SGD and Adam

Model Architecture	Momentum	Adam
ConvNet	$12.86_{\pm 4.66}$	$\mathbf{16.12_{\pm 7.98}}$
ResNet-20	$\mathbf{11.00_{\pm 0.52}}$	$10.09_{\pm 0.15}$

I.2.2 Vision Transformer for PACS

Vision Transformer (ViT)(Dosovitskiy et al., 2020) is a neural network using the recent attention structure. We evaluated the out-of-distribution performance when using Vision Transformer as well as ResNet-50 used in DomainBed. However, due to computational resource constraints, we compared Adam and Momentum SGD only for the task on the PACS dataset. The experimental results are shown in Table 18.

As a result, the experimental results with Vision Transformer show a significant performance improvement over the ResNet-50 case. Furthermore, the result that Momentum SGD outperforms Adam is consistent with the ResNet-50 case.

Table 18: PACS: OOD accuracy(%) comparison between Momentum SGD and Adam

Model Architecture	Momentum	Adam
ResNet-50	**87.03**$_{\pm 0.65}$	83.94$_{\pm 0.88}$
ViT	**90.28**$_{\pm 0.54}$	90.05$_{\pm 0.29}$

I.3 State-of-the-Arts Optimizers

I.3.1 Sharpness Aware Minimization (SAM)

Sharpness-Aware Minimization (SAM) (Foret et al., 2020) prevents convergence to high curvature local minima. Its convergence towards smaller curvature solutions results in high validation and test performance on in-distribution (ID) environment. SAM searches for points where the loss is maximized within a neighborhood of ρ and uses the gradient at that point for iterative optimization. The larger the ρ, the higher the effect of preventing convergence to high curvature local minima.

We carried out experiments with SAM on PACS and Amazon-WILDS datasets tasks, comparing it to both Momentum SGD and Adam over a range of hyperparameters outlined in Appendices E.3 and E.3. The experimental results indicated competitive performance by SAM, equaling Momentum SGD. In the case of the Amazon-WILDS dataset, SAM proved superior for both in-distribution and out-of-distribution accuracy.

Table 19: PACS: Accuracy (%) comparison of SAM with Momentum SGD and Adam

Accuracy	Momentum	Adam	SAM
ID accuracy	96.79$_{\pm 0.9}$	96.78$_{\pm 0.42}$	**97.54**$_{\pm 0.07}$
OOD accuracy	**87.03**$_{\pm 0.65}$	83.94$_{\pm 0.88}$	86.65$_{\pm 0.9}$

Table 20: Amazon-WILDS: Accuracy (%) comparison of SAM with Momentum SGD and Adam

Accuracy	Momentum	Adam	SAM
ID accuracy	72.51$_{\pm 0.06}$	72.02$_{\pm 0.07}$	**73.42**$_{\pm 0.07}$
OOD accuracy	53.33$_{\pm 0.0}$	52.67$_{\pm 0.77}$	**54.0**$_{\pm 0.94}$

I.3.2 Adam with Decoupled Weight Decay (AdamW)

The AdamW optimizer, proposed by Loshchilov & Hutter (2017) is an extension of the popular Adam optimization algorithm. AdamW addresses the shortcomings of the original Adam optimizer concerning weight decay regularization. In the original Adam algorithm, weight decay is directly applied to the adaptive learning rates, causing a discrepancy between the intended effect of weight decay and the actual effect in practice. The AdamW optimizer decouples weight decay from the adaptive learning rates, resulting in a more effective regularization method that is better suited for various deep learning tasks. By incorporating weight decay separately from the update step, the AdamW optimizer exhibits improved convergence properties and generalization performance compared to the original Adam algorithm.

We show the results of our AdamW experiment in Table 21. After tuning learning rate and selecting the model with the best learning rate, we ran the experiment with three different seeds and computed the mean and variance. We found that AdamW performs better than Adam, but not as well as Momentum SGD.

Table 21: Amazon-WILDS: Comparison of AdamW with Momentum SGD and Adam

Accuracy	Momentum	Adam	AdamW
ID accuracy	**72.51**$_{\pm 0.06}$	72.02$_{\pm 0.07}$	72.27$_{\pm 0.21}$
OOD accuracy	**53.33**$_{\pm 0.0}$	52.67$_{\pm 0.77}$	**53.33**$_{\pm 0.33}$

I.4 Large ϵ for Adam

The study in Choi et al. (2019) shows that high in-distribution performance similar to Momentum SGD can be achieved with large ϵ. However, ϵ is a hyperparameter that has been introduced to prevent zero-percentage, and is specified as ϵ = 1e-8 in pytorch's default implementation[8]. It is known that as ϵ increases, Adam approximate Momentum SGD (Choi et al., 2019). While this section of our paper investigated with ϵ to the extent that it behaves as Adam, in this section we provide experimental results at large ϵ, where Adam is expected to behave more like Momentum SGD.

The results of the experiment are shown in Figure 49. The x marker in the lower left corner shows the results for the default hyperparameters in Adam. The other circle markers are for different ϵ in Adam. Red stars indicate some of the Momentum results. It can be seen that the larger ϵ achieved performance closer to Momentum SGD than the default ϵ in Adam.

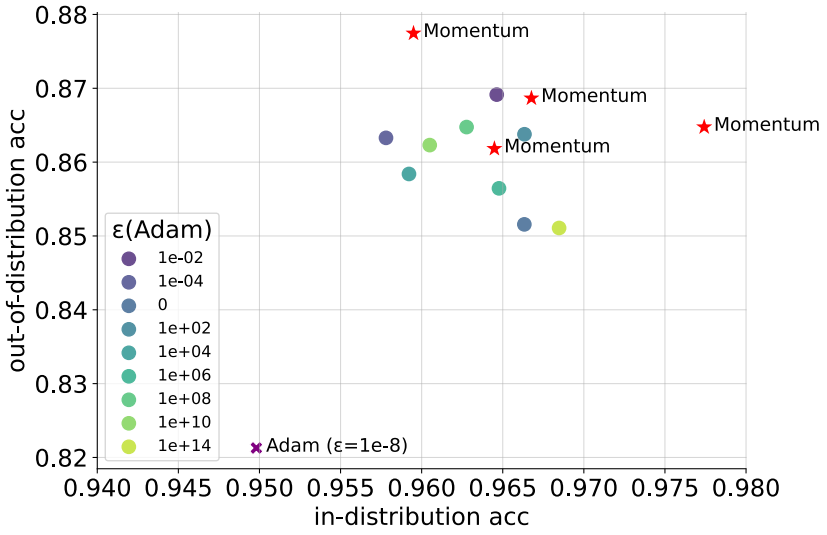

Figure 49. Demonstrating the varying performance of out-of-distribution accuracy according to the value of ϵ in Adam. As ϵ becomes larger, it approaches the performance of Momentum.

I.5 Learning Rate Schedule

Amazon-WILDS task uses linear scheduling without warmups [9]. However, learning rate scheduling can affect performance. To consider this impact, we compared and verified the following four learning rate schedules and eight patterns with and without warmup.

Table 22 shows the results of the Amazon-WILDS experiments. However, the results for the largest out-of-distribution accuracy are shown since no significant differences were found for all experiments. No significant differences were found with or without warmup. It was not clear that introducing warmup is always effective. The Cosine LR Schedule was found to be the most effective in the problem setting of this study.

[8] https://pytorch.org/docs/stable/generated/torch.optim.Adam.html
[9] https://github.com/p-lambda/wilds

Table 22: Amazon-WILDS: OOD Accuracy (%) comparison of LR Scheduler and Warmup

Learning Rate Schedule	Momentum	Adam	AdamW
Constant LR	53.33	53.33	52.00
Constant LR + Warmup	53.33	52.00	53.33
Cosine LR	**54.67**	**54.67**	**54.67**
Cosine LR + Warmup	**54.67**	**54.67**	**54.67**
Linear LR (Default)	**54.67**	52.00	52.00
Linear LR + Warmup	**54.67**	**54.67**	53.33
MultiStep LR	52.00	53.33	52.00
MultiStep LR + Warmup	50.67	53.33	52.00

The CivilComments-WILDS task, akin to Amazon-WILDS, employs linear scheduling without warmups, as elucidated in the official repository[10]. We proceeded to examine the CivilComments-WILDS dataset to identify any analogous trends that may emerge. Our analyses from the CivilComments-WILDS dataset corroborated the findings from our Amazon-WILDS study, thereby reinforcing our preliminary conclusion that non-adaptive optimizers typically exhibit superior performance over their adaptive counterparts. Notably, we observed a significant deviation in the OOD performance when modifying the learning rate scheduler in the CivilComments-WILDS dataset. This observation starkly contrasts with our experiences in the Amazon-WILDS setting. Moreover, despite these modifications to the learning rate scheduler, we could not surpass the performance outcomes achieved with the default learning rate schedule. This reiterates the efficacy of the default setting, and further validates our overall findings.

Table 23: CivilComments-WILDS: OOD Accuracy (%) comparison of LR Scheduler and Warmup

Learning Rate Schedule	Momentum	Adam
Constant LR	47.82	44.29
Constant LR + Warmup	47.54	44.44
Cosine LR	56.98	45.40
Cosine LR + Warmup	56.83	45.48
Linear LR (Default)	**57.69**	**46.82**
Linear LR + Warmup	57.14	45.00
MultiStep LR	47.82	44.29
MultiStep LR + Warmup	51.35	44.04

I.6 The Effect of Random Seeds

We conducted experiments on the effect of seed, which controls randomness, such as model initialization, on learning, using the PACS and Amazon-WILDS datasets.

In the PACS experiment shown in Table 24, a performance difference of around 6% was observed due to the effect of seed, especially for Adam. In contrast, in Momentum SGD, the effect of seed was not significant. In the Amazon-WILDS experiment shown in Table 25, seed had no significant effect on either Adam or Nesterov Momentum SGD.

Table 24: PACS: OOD Accuracy (%) Different Seed Comparison

Seed	Momentum	Adam
2021	86.47	81.20
2022	86.47	87.06
2023	87.74	85.69

Table 25: Amazon-WILDS: OOD Accuracy (%) Different Seed Comparison

Seed	Nesterov	Adam
2021	53.33	52.00
2022	53.73	53.33
2023	54.67	53.33

[10] https://github.com/p-lambda/wilds

I.7 Algorithms (ERM, IRM, VREx and CORAL)

In this study, we focused on ERM and IRM and obtained consistent results that the Non-Adaptive optimizer outperforms the Adaptive optimizer in out-of-distribution performance. We also verified the use of VREx(Krueger et al., 2021) and CORAL(Sun & Saenko, 2016) as the other algorithms. The results of these experiments are shown in Table 26. However, due to limited computing resources, experiments were conducted only for Momentum SGD and Adam for PACS.

Table 26: PACS: OOD Accuracy (%) comparison of algorithms (ERM, IRM, VREx and CORAL)

Algorithm	Momentum	Adam
ERM	**87.03**$_{\pm 0.65}$	83.94$_{\pm 0.88}$
IRM	**83.06**$_{\pm 0.32}$	83.05$_{\pm 0.44}$
VREx	**85.70**$_{\pm 0.24}$	84.85$_{\pm 1.88}$
CORAL	**84.25**$_{\pm 1.35}$	84.10$_{\pm 1.13}$